

Pacific Northwest National Laboratory

Operated by Battelle for the
U.S. Department of Energy

Investigation of Flammable Gas and Thermal Safety Issues for Retrieval of Waste from Tank 241-AN-105

C. M. Caley
S. W. Stewart
Z. I. Antoniak

J. M. Cuta
L. A. Mahoney
F. E. Panisko

RECEIVED
SEP 28 1998
OSTI

September 1998

Prepared for the U.S. Department of Energy
under Contract DE-AC06-76RLO 1830

MASTER *JAT*

DISTRIBUTION OF THIS DOCUMENT IS UNLIMITED

DISCLAIMER

This report was prepared as an account of work sponsored by an agency of the United States Government. Neither the United States Government nor any agency thereof, nor Battelle Memorial Institute, nor any of their employees, makes any warranty, express or implied, or assumes any legal liability or responsibility for the accuracy, completeness, or usefulness of any information, apparatus, product, or process disclosed, or represents that its use would not infringe privately owned rights. Reference herein to any specific commercial product, process, or service by trade name, trademark, manufacturer, or otherwise does not necessarily constitute or imply its endorsement, recommendation, or favoring by the United States Government or any agency thereof, or Battelle Memorial Institute. The views and opinions of authors expressed herein do not necessarily state or reflect those of the United States Government or any agency thereof.

PACIFIC NORTHWEST NATIONAL LABORATORY

operated by

BATTELLE

for the

UNITED STATES DEPARTMENT OF ENERGY

under Contract DE-AC06-76RLO 1830

Printed in the United States of America

Available to DOE and DOE contractors from the
Office of Scientific and Technical Information, P.O. Box 62, Oak Ridge, TN 37831;
prices available from (615) 576-8401.

Available to the public from the National Technical Information Service,
U.S. Department of Commerce, 5285 Port Royal Rd., Springfield, VA 22161



This document was printed on recycled paper.

DISCLAIMER

This report was prepared as an account of work sponsored by an agency of the United States Government. Neither the United States Government nor any agency thereof, nor any of their employees, makes any warranty, express or implied, or assumes any legal liability or responsibility for the accuracy, completeness, or usefulness of any information, apparatus, product, or process disclosed, or represents that its use would not infringe privately owned rights. Reference herein to any specific commercial product, process, or service by trade name, trademark, manufacturer, or otherwise does not necessarily constitute or imply its endorsement, recommendation, or favoring by the United States Government or any agency thereof. The views and opinions of authors expressed herein do not necessarily state or reflect those of the United States Government or any agency thereof.

DISCLAIMER

Portions of this document may be illegible in electronic image products. Images are produced from the best available original document.

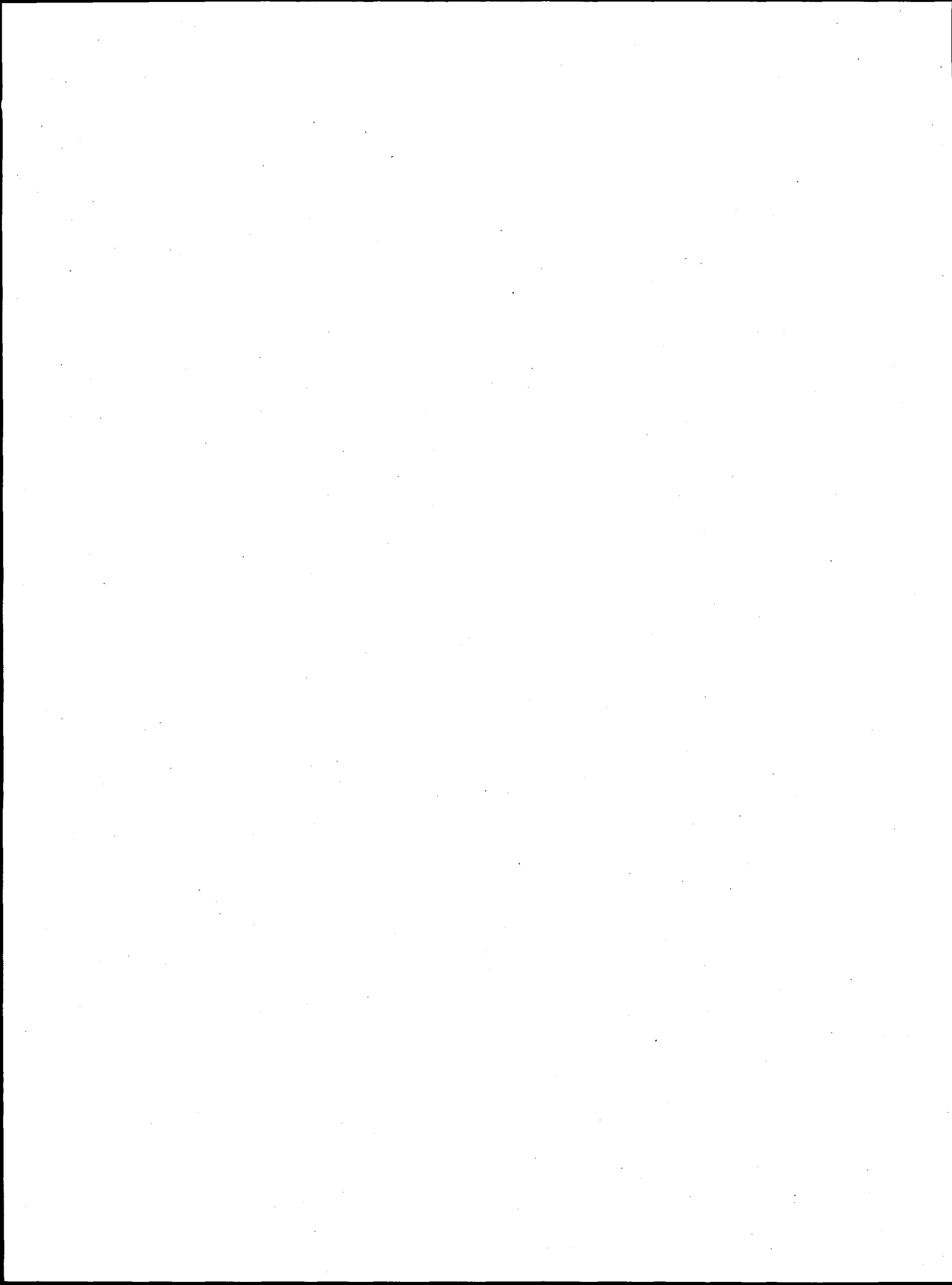
**Investigation of Flammable Gas
and Thermal Safety Issues
for Retrieval of Waste from
Tank 241-AN-105**

S.M. Caley
C.W. Stewart
Z. I. Antoniak
J. M. Cuta
L.A. Mahoney
F.E. Panisko

September 1998

Prepared for
the U.S. Department of Energy
under Contract DE-AC06-76RLO 1830

Pacific Northwest National Laboratory
Richland, WA 99352



Summary

The primary purpose of this report is to identify and resolve some of the flammable gas and thermal safety issues potentially associated with the retrieval of waste from Tank 241-AN-105 (AN-105), which is the first double-shell tank scheduled for waste retrieval at Hanford. The planned retrieval scenario includes the following steps in AN-105: 1) degas the tank using two submerged mixing pumps, 2) turn off the mixer pump(s) and allow any suspended solids to settle, 3) decant the supernatant to the intermediate feed staging tank(s) (IFSTs) (AP-102 and/or AP-104) using water/caustic dilution at the transfer pump inlet, 4) add the remaining dilution water/caustic to the slurry remaining in AN-105, 5) mix the tank with the mixer pump(s) until the soluble solids dissolve, 6) turn off the mixer pump(s) and let the insoluble solids settle, and 7) decant the "new" supernatant to the IFST(s), leaving the insoluble solids behind.

Three waste retrieval safety issues are addressed in this report. They are 1) the controlled degassing of AN-105 to ensure that the headspace remains <25% of the lower flammability limit (LFL), 2) an assessment of how dissolved gas (mainly ammonia) released during the transfer of the supernatant in AN-105 to the IFSTs and the water/caustic dilution of the remaining slurry in AN-105 will affect the flammability in these tanks; and 3) an assessment of the maximum waste temperatures that might occur in AN-105 during retrieval operations.

Degassing Plan

The goal of the degassing phase of waste retrieval is to remove the bulk of the stored gas from the tank, reducing or eliminating the flammable gas safety hazard prior to subsequent retrieval steps. During degassing, the gas release rate will be controlled to ensure that the flammable gas mixture present in the tank headspace remains <25% of the LFL. Degassing will be accomplished by gently mixing the waste with two submerged mixing pumps. The efficacy of a mixer pump in removing stored gas and preventing episodic gas releases has been demonstrated in Tank SY-101 and this experience was used to develop the AN-105 degassing plan.

To ensure that the gas release in AN-105 proceeds in small increments and that the headspace remains well below the flammability limit, it is proposed that the pumps be operated one at a time, in a fixed direction, at their lowest operating speed of 700 rpm, and for limited run times of 24 minutes. The pump run time was based on the maximum gas release volume measured during SY-101 mitigation, 14.3 m³ (508 ft³), which is less than the calculated, instantaneous release volume in AN-105 of 16.8 m³ (590 ft³) that would bring the headspace to 25% of the LFL. The maximum daily gas release during SY-101 mitigation occurred on November 5, 1993 during Phase B test B-5. The calculated energy supplied by the pump to the waste during test B-5 was approximately 18.2 kW-hr (24.4 hp-hr). One of the W-211 pumps operating at 700 rpm would supply this same amount of energy to AN-105 waste in approximately 24 minutes.

During degassing, it is recommended that the pump in riser 008 be used during the first pump run, with the nozzles N-S at 0-180 degrees. The second pump run will then use the pump in riser 007, with its nozzles N-S at 0-180 degrees. Subsequent runs should alternate pump use and vary the nozzle directions by 45°. Based on SY-101 experience, a one-day wait time should be enforced between pump runs to ensure that any delayed gas releases occur before the next run. A complete tank sweep using both pumps should be accomplished in a minimum of eight days,

assuming there are no alarms causing pump operation to be aborted or other delays due to weather, etc. Pump runs will continue until it is assessed that sufficiently little stored gas remains in AN-105 to permit continuous operation of both pumps without exceeding 25% of the LFL. Gas chromatographs (GCs) measure hydrogen and other gases in the tank headspace and these concentrations can be multiplied by the ventilation flowrate and integrated over time to determine the cumulative amount of gas removed beyond the baseline or background release rate.

Dissolved Gas Release

The flammable gas modeling approach developed in Peurrung et al. (1998) for analysis of the double-contained receiver tanks (DCRTs) was used to determine how much dissolved gas (mainly ammonia) would be released during the process of diluting the AN-105 supernatant with water/caustic and pumping the liquid out of AN-105 into the IFSTs AP-102 and AP-104. Two different models, an "equilibrium" model and a "non-equilibrium" model, were used to estimate the ammonia levels in the tank headspaces for two different scenarios:

Case 1 -- 1,890 kL (500 kgal) of undiluted supernatant from AN-105 is transferred to AP-102; this represents the initial transfer of existing liquid and potentially represents the highest headspace flammability in the receiver tank.

Case 2 -- 3,822 kL (1,011 kgal) of waste resulting from 80% dilution of settled solids with water is mixed in AN-105; this case explores the extent to which dilution and the absence of a crust affects the headspace flammability in the source tank.

Both the equilibrium and nonequilibrium models predict that the ammonia in the AP-102 headspace over the undiluted supernatant (Case 1) will not pose a flammability hazard; the levels are only estimated to be 4 to 4.5% of the LFL. The maximum flammability in the AP-102 headspace occurs immediately after filling, and the flammability decreases with subsequent ventilation. When the waste solids in AN-105 are 80% diluted (Case 2), these models predict that the maximum ammonia concentration in the AN-105 headspace over the diluted waste will be approximately 1.6% of the LFL, which again is significantly less than the 25% LFL safety limit.

Maximum Waste Temperatures

A two-dimensional model developed for determining heat transfer in SY-101 using the TEMPEST computer code was modified to predict AN-105 waste temperatures for variable waste layer depths, conditions, and compositions that might occur during retrieval operations. Initial steady-state thermal modeling of AN-105 behavior predicted waste temperatures that closely corresponded to measured values, suggesting that the assumptions made for waste composition, properties, and vent air flows in the thermal model were valid and that the existing knowledge of AN-105 waste was sufficient for further analyses.

Two additional simulations were performed. The first was a 180-day cooling period for a post-mixed AN-105. This simulation assumed that the mixed waste was at a uniform temperature

of 82.2°C (180°F) and predicted that at the end of the 180-day cooldown period the tank contents would still be quite hot: the nonconvective waste at a maximum temperature of 76°C (169°F) and the convective waste at a near-uniform temperature of 62°C (143°F).

The 180-day cooling simulation was repeated, assuming a "fluffing factor" of 1.8 for the nonconvective waste in AN-105. The reason for assuming a "fluff factor" is that after mixing, tank waste does not settle to the same level it was before mixing because of entrained liquid. It can take several months, even up to a year before the waste level is reduced to its original height. Bench-scale tests and computer simulations of other tanks suggest that the nonconvective volume increase may be in the range of 1.4 to 1.8 times the original volume. This increase in volume increases the thermal conduction path length through the nonconvective waste and therefore has a large impact on calculated peak steady-state temperatures.

The temperature profiles for the run with a 1.8 "fluffing factor" paralleled those of the run without a "fluffing factor", except that the nonconvective layer temperature rose to a peak of nearly 86.1°C (186.9°F) after 150 days of cooling and at the end of the 180-day cooldown period had only cooled to 85.9°C (186.6°F). The convective layer temperature cooled to a near-uniform 48°C (119.9°F) during the 180-day cooldown period.

The second TEMPEST simulation evaluated steady-state thermal conditions both before and after AN-105 supernatant decant to an IFST. The predicted steady-state temperatures of the waste remaining after supernatant decant were low, with peak waste temperatures between ~33 and 53°C (91 and 128°F), depending on the "fluffing factor" assumed for the nonconvective layer. For the scenario where supernatant decant does not take place after mixing, the peak waste temperature for a 1.8 "fluff" case was calculated to be 57°C (134°F). For all the TEMPEST simulations performed, AN-105 waste temperatures were predicted to remain well below safety limits, even with the conservative assumptions made.

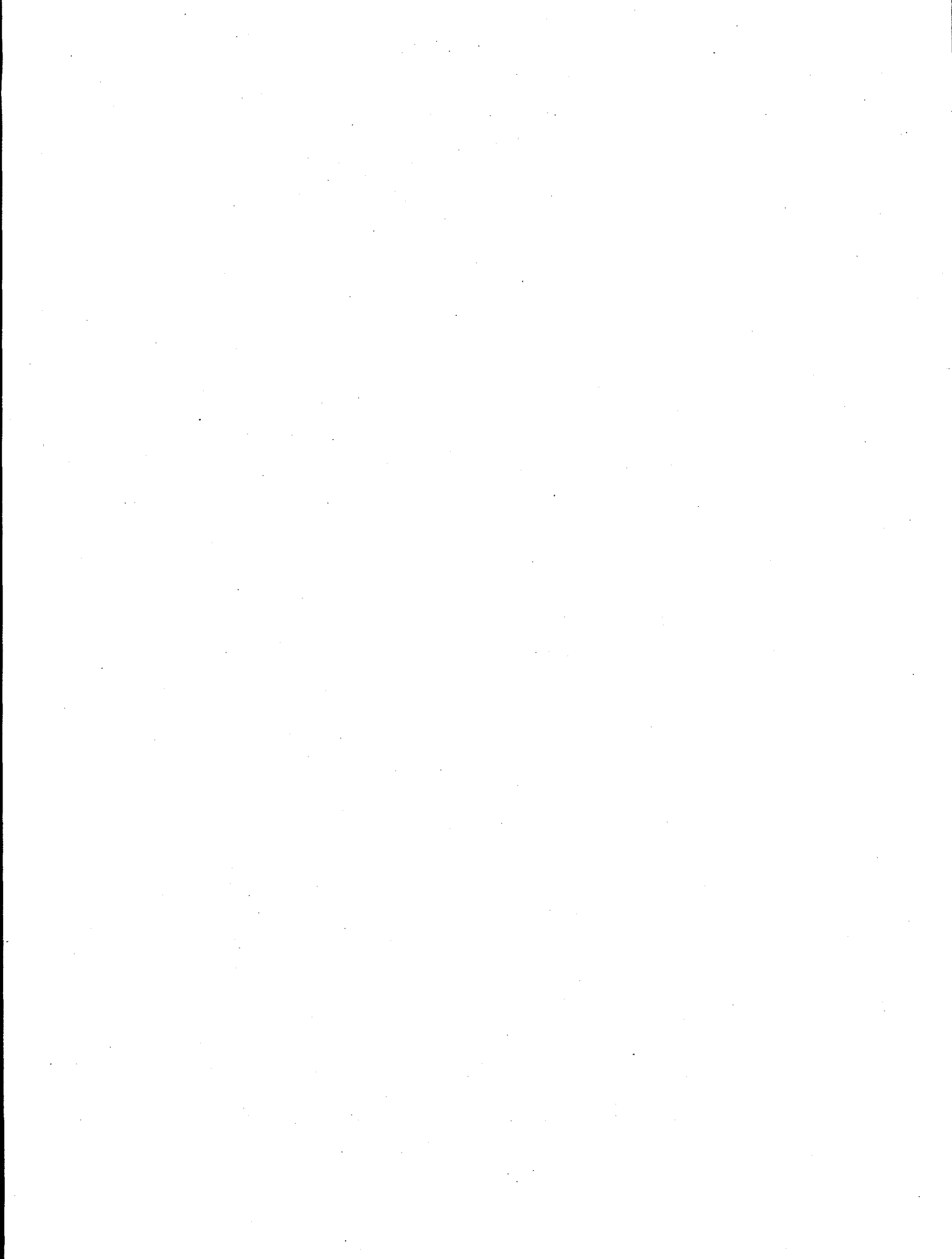
Conclusions

Based on the three investigations described above, we conclude that

- AN-105 waste can be degassed safely, that is, without exceeding 25% of the LFL in the tank headspace.
- Dissolved ammonia in AN-105 waste poses no flammability threat during supernatant dilution and transfer.
- AN-105 waste temperatures should remain below safety limits during retrieval activities.

Reference

Peurrung, LM, LA Mahoney, CW Stewart, PA Gauglitz, LR Pederson, SA Bryan, and CL Shepard. 1998. *Flammable Gas Issues in Double-Contained Receiver Tanks*. PNNL-11836 Rev. 2, Pacific Northwest National Laboratory, Richland, Washington.



Contents

Summary.....	iii
1.0 Introduction.....	1.1
2.0 Degassing Plan	2.1
2.1 Summary of Tank SY-101 Mitigation Experience.....	2.1
2.2 Comparison of SY-101 and AN-105 Waste	2.3
2.3 Comparison of SY-101 and W-211 Pump Designs.....	2.5
2.4 AN-105 Degassing Strategy	2.12
2.5 Monitoring and Control.....	2.17
3.0 Dissolved Gas Release	3.1
3.1 Input Parameters and Boundary Conditions	3.2
3.2 Results.....	3.5
4.0 Maximum Waste Temperatures.....	4.1
4.1 Thermal Modeling Approach.....	4.1
4.2 Parametric Study to Determine Initial Conditions	4.4
4.3 Simulation of the Cooldown of a Hot, Mixed Tank.....	4.6
4.4 Simulation of Steady-State after Supernatant Decant.....	4.8
4.5 Summary and Conclusions.....	4.11
5.0 References	5.1

Figures

2.1	Peak Hydrogen Concentration and Waste Surface Level During SY-101 Phase B Pump Operations	2.2
2.2	Daily Gas Release and Waste Surface Level During SY-101 Phase B Pump Operations	2.2
2.3	Schematic of the SY-101 and W-211 Mixer Pumps.....	2.7
2.4	Maximum Retained Bubble Diameter vs. Yield Stress	2.8
2.5	Plan View of Tank SY-101.....	2.10
2.6	Plan View of Tank AN-105	2.10
2.7	Comparison of SY-101 and W-211 Mixer Pump Performance	2.11
2.8	Pump Flow Power vs. Pump Speed for SY-101 and W-211 Mixer Pumps	2.12
2.9	Proposed Pump Run Schedule for AN-105 Degassing	2.15
2.10	Temperature Trends at Riser 17B During a SY-101 Jet Penetration Test	2.16
4.1	Schematic of the Model Domain	4.2
4.2	Measured and Calculated Temperature Comparison for Tank AN-105	4.5
4.3	Calculated Steady-State Temperature Contours for Tank AN-105.....	4.6
4.4	Calculated Transient Temperatures for Tank AN-105 Cooldown.....	4.7
4.5	Calculated Steady-State Temperature Contours for AN-105 Waste after Supernatant Decant; Upper Frame = "Fluff Factor" of 1, Lower Frame = "Fluff Factor" of 1.4	4.9
4.6	Calculated Steady-State Temperature Contours AN-105 Waste with a "Fluff Factor" of 1.8; Upper Frame = After Supernatant Decant, Lower Frame = Before Supernatant Decant	4.10

Tables

2.1	Physical Properties of SY-101 and AN-105 Waste.....	2.4
2.2	Waste Gas Composition in Tanks SY-101 and AN-105.....	2.4
2.3	Nonconvective Layer Flammability Summary for Tanks SY-101 and AN-105.....	2.5
2.4	Design Parameters of the SY-101 and W-211 Mixing Pumps	2.6
3.1	Model Input Parameters.....	3.3
3.2	AN-105 Flammability Analysis for Postulated Cases of Liquid Waste Transfer and Dilution.....	3.6
4.1	Summary of Conditions and Material Properties for Tank AN-105	4.3
4.2	Bottom Air Channel Heat Transfer Coefficients	4.4
4.3	Results of the Annulus Air Flow Sensitivity Analysis	4.5

1.0 Introduction

There are 177 underground waste storage tanks on the Hanford Site; 149 of these are single-shell tanks (SSTs) and 28 are double-shell tanks (DSTs). The waste in most of the tanks generates flammable gas, mainly hydrogen, along with ammonia, methane, the oxidizer nitrous oxide, and inert nitrogen (King et al. 1997). In some of the waste tanks these flammable gases are known or suspected to be retained in significant quantities (Hanlon 1995). Because of the potential for gas releases and resulting flammable headspace conditions, 25 tanks have been placed on the Flammable Gas Watch List (FGWL), including six DSTs (SY-101, SY-103, AW-101, AN-103, AN-104, and AN-105).^(a)

The flammable gas hazard in Hanford waste tanks was made an issue by the behavior of DST SY-101. Shortly after SY-101 was filled in 1980, the waste level began periodically rising, due to the generation and retention of gases within the slurry, and then suddenly dropping as the gases were released. Between 1990 and 1992, an intensive study of the tank's behavior revealed that these episodic gas releases posed a safety hazard because the released gas was flammable and the releases were quite large (Allemann et al. 1993). In fact, some of the gas releases had sufficient volume to exceed the lower flammability limit (LFL) in the entire tank headspace. A mixer pump was installed in SY-101 in late 1993 to prevent gases from building up in the settled solids layer and the large episodic gas releases have since ceased (Allemann et al. 1994; Stewart et al. 1994; Brewster et al. 1995). This experience with SY-101 caused a concern that other tanks might have similar large gas releases or have the potential for such releases; however, current theory and monitoring data suggest that the large episodic gas releases in SY-101 were unique in both size and hazard (Meyer et al. 1997).

The historic gas releases in SY-101 prior to mixing were buoyancy-induced displacement events,^(b) where a portion, or "gob," of the nonconvective layer near the tank bottom accumulated enough gas to become buoyant and overcame the weight and strength of the material restraining it, thereby breaking away and rising through the supernatant layer (Allemann et al. 1993). The stored gas bubbles expand as the waste rises, causing the surrounding matrix to fail and a portion of the gas to escape from the gob into the headspace. Theory, experiment, and experience indicate that only the DST waste configuration of a settled solids layer under a relatively deep layer of supernatant liquid has the potential for significant gas releases by buoyant displacements (Stewart et al. 1996). The five other DSTs on the FGWL (SY-103, AW-101, AN-103, AN-104, and AN105) each exhibit this kind of episodic gas release; however, these releases are typically less than 30 cubic meters in volume, compared with over 100 cubic meters in SY-101 prior to mitigation (Meyer et al. 1997).

The first DST scheduled for waste retrieval is Tank AN-105. The planned retrieval scenario includes the following steps: 1) degas the tank using two submerged mixing pumps, 2) turn off the mixer pump(s) and allow any suspended solids to settle, 3) decant the supernatant to the intermediate feed staging tank(s) (IFSTs) (AP-102 and/or AP-104) using water/caustic dilution at the transfer pump inlet, 4) add the remaining dilution water/caustic to the slurry remaining in

(a) Waste tanks are formally denoted with a "241-" prefix, for example, "241-SY-101." The "241-" has been removed per common usage.

(b) Buoyant displacements were historically, though incorrectly, termed "rollovers" (Meyer et al. 1997).

AN-105, 5) mix the tank with the mixer pump(s) until the soluble solids dissolve, 6) turn off the mixer pump(s) and let the insoluble solids settle, and 7) decant the "new" supernatant to the IFST(s), leaving the insoluble solids behind.

The primary purpose of this report is to identify and resolve some of the flammable gas and thermal issues potentially associated with the retrieval of AN-105 waste. Section 2 describes the degassing plan, which was modeled after the SY-101 mixer pump operations. The goal of the degassing phase of AN-105 waste retrieval is to remove the bulk of the stored gas from the tank at a controlled rate so as not to exceed 25% of the LFL in the tank head space.

Section 3 presents modeling results that evaluated how much dissolved gas (mainly ammonia) would be released during the dilution and transfer of AN-105 supernatant waste. The purpose of this evaluation was to confirm that flammability levels in the headspaces of AN-105 and the IFSTs, AP-102 and AP-104, remain at less than 25% of the LFL.

Section 4 presents results from a two-dimensional thermal computer model of Tank AN-105 that was developed to predict waste temperatures for variable waste layer depths, conditions, and compositions that might occur during retrieval operations. The purpose of this analysis was to confirm that AN-105 waste temperatures remain at less than safety limits during various retrieval activities.

2.0 Degassing Plan

The goal of the degassing phase is to remove the bulk of the stored gas from the tank, reducing or eliminating the flammable gas safety hazard during the succeeding phases of retrieval.^(a) During degassing, gas releases will be controlled to ensure that the flammable gas mixture present in the tank dome space remains at <25% of the LFL. Degassing will be accomplished by gently mixing the waste with two submerged mixing pumps. Intermittent mixing mobilizes a controlled volume of gas-bearing waste, releasing a large fraction of the gas it contains. The pump run time has been computed to ensure the gas release proceeds in small increments to keep the headspace well below the 25% LFL limit. The efficacy of a mixer pump in preventing episodic gas releases has been demonstrated in SY-101 and this experience was used to develop the AN-105 degassing plan.

A summary of the SY-101 mitigation experience is presented in Section 2.1. Sections 2.2 and 2.3 compare SY-101 and AN-105 waste and pump designs, respectively. Finally, Section 2.4 outlines the AN-105 degassing strategy, and Section 2.5 discusses the data monitoring and control strategy recommended for the degassing process.

2.1 Summary of Tank SY-101 Mitigation Experience

A spare mixing pump from the Grout Program was modified and installed in Tank SY-101 on July 3, 1993. The purpose of the mixing pump was to prevent the large, episodic flammable gas releases that had been occurring in the tank about every 100-150 days (Babad et al. 1992; Antoniak 1993). Initial pump operations (Phase A) were extremely gentle because of concerns that pump operation might trigger a major gas release event (GRE). This initial, low-speed testing continued through October of 1993 and did very little to disturb the waste or release gas, but it did show that brief pump operations called "bumps" were required about every other day to prevent nozzle plugging (Allemann et al. 1994).

High-speed mixer pump testing (Phase B) began on October 21, 1993 and continued until December 17, 1993. Phase B consisted of a series of tests where the pump run time varied from 20 to 30 minutes with the pump speed between 360 and 920 rpm (Allemann et al. 1994). The primary measures of success for the SY-101 mixer pump testing were to maintain the maximum hydrogen concentration in the dome space well below 25% of the LFL^(b) and to keep the waste level at an acceptably low value^(c) for an extended period of time. Figure 2.1 shows the daily peak hydrogen concentrations and the waste surface level during Phase B testing (Allemann et al. 1994). Figure 2.2 shows the daily total volume of gas released during Phase B testing.^(d) For comparison, the baseline gas generation rate is approximately 3 m³/day (106 ft³/day) (Stewart et al. 1994). As shown in both figures, a large volume of retained gas was released during the first few weeks of testing, and the waste level was reduced to a historic low of approximately 1016 cm (400 in.).

(a) Degassing only removes stored gas; it does not alter gas generation. Therefore, gas could re-accumulate if there were protracted delays (i.e., several months) after degassing.

(b) The LFL for hydrogen is 4 volume percent (40,000 parts per million [ppm]) in air (Cashdollar et al. 1992).

(c) Waste level changes, accounting for waste transfers and evaporation, are a measure of gas retention and release.

(d) The gas release was calculated by integrating the hydrogen concentration times the flow rate each day and dividing by an assumed hydrogen fraction of 0.29 in the released gas.

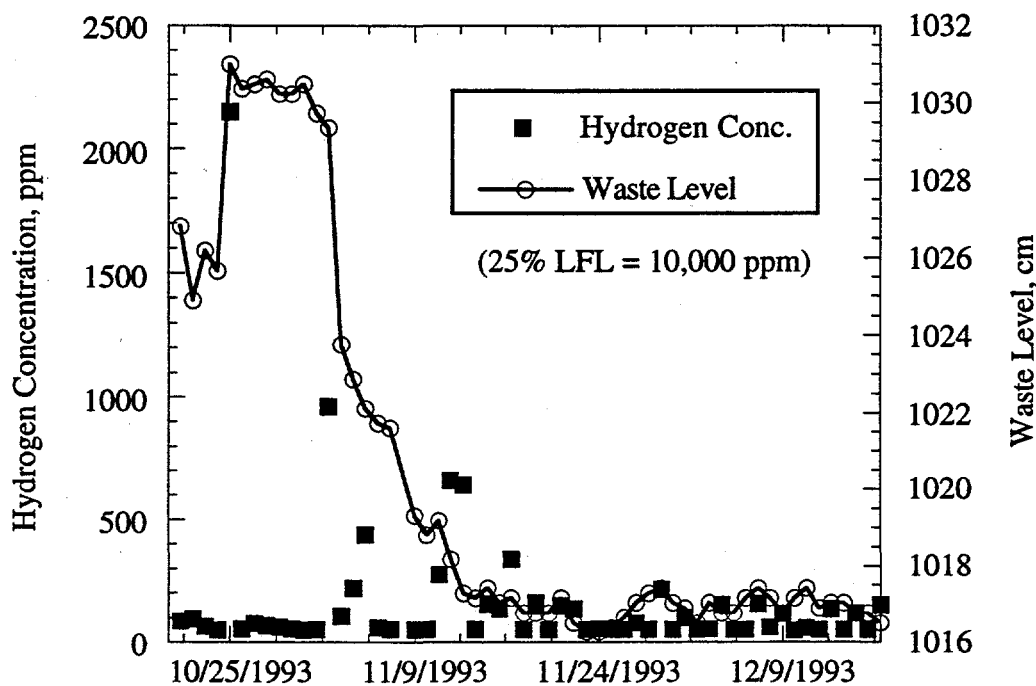


Figure 2.1. Peak Hydrogen Concentration and Waste Surface Level During SY-101 Phase B Pump Operations

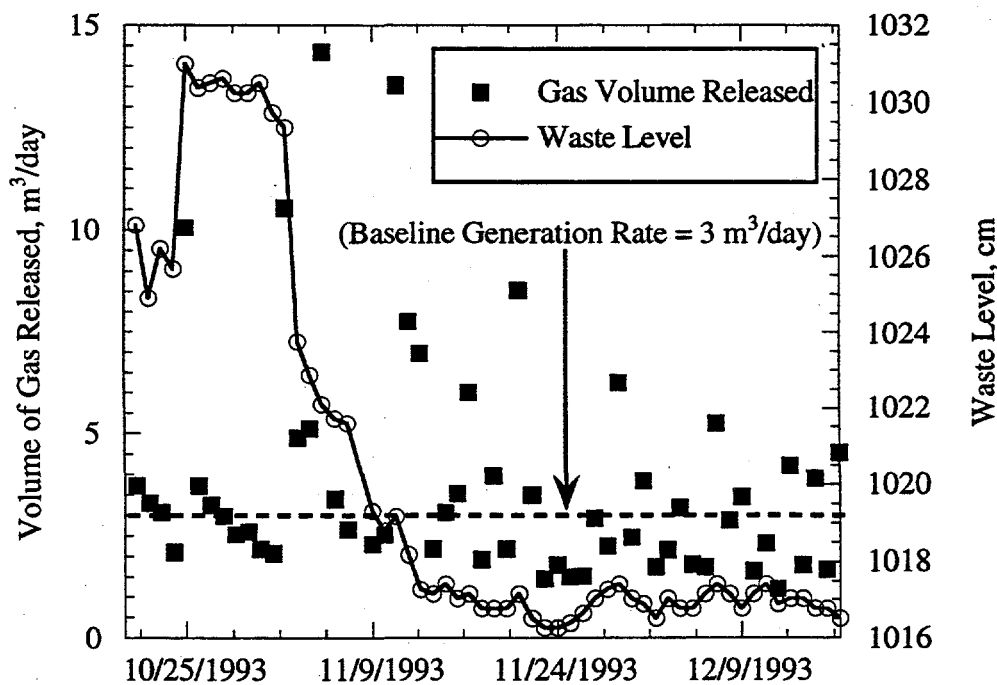


Figure 2.2. Daily Gas Release and Waste Surface Level During SY-101 Phase B Pump Operations

By early December, the jets had apparently mixed most of the gas-bearing nonconvective layer because gas releases for the remainder of Phase B testing were relatively small.

Mitigation of Tank SY-101 was considered successful after completion of Phase B testing. From late November of 1993 until the end of Phase B testing, the hydrogen concentration remained below 400 ppm and the waste level remained below 1021 cm (402 in.). In addition, the uniform vertical temperature profiles at two in-tank thermocouple trees showed that the waste was well mixed except for approximately 127 cm (50 in.) of waste at the bottom (Allemann et al. 1994). This success enables us to model the degassing of AN-105 after SY-101's Phase B pump operations. In order to do this, the waste in Tank AN-105 was compared with the waste in Tank SY-101 and the design of the W-211 Pump (the mixer pump that will be used during waste retrieval in AN-105) was compared with the design of the SY-101 mixer pump. These comparisons are presented in Sections 2.2 and 2.3.

2.2 Comparison of SY-101 and AN-105 Waste

Tank SY-101 is a double-shell, high-level radioactive waste tank located in the 200 West Area on the Hanford Site. The tank was designed for use as a concentrated waste holding tank and went into service in 1977 with the receipt of double-shell slurry from the 242-S Evaporator. From 1977 to 1980, SY-101 received periodic transfers of double-shell slurry, in addition to concentrated complexant waste originally from B Plant, and a small amount of water (Herting et al. 1995). Shortly after the first waste was added to SY-101, the waste began to exhibit slurry growth caused by the generation and retention of gases. Until the mixer pump was installed in 1993, the waste followed a pattern of steady slurry growth with sudden episodic volume decreases as large volumes of gas were released (Allemann et al. 1993).

Tank AN-105 is a double-shell, high-level radioactive waste tank located in the 200 East Area on the Hanford Site. The tank went into service in 1981, receiving water, and continued to receive water until November 1982. The tank received double-shell slurry feed waste from AW-102 from December 1982 until the second quarter of 1983 and received noncomplexed waste from AN-104 in the first quarter of 1984. Most of this waste was removed during the first quarter of 1985 for evaporator campaign, leaving approximately 154 kgal waste in AN-105. During the first and second quarters of 1985, the tank received double-shell slurry feed waste from AW-102 via the evaporator, then waste reception ceased (Jo 1997).

An estimate of the waste constituents of SY-101 was developed from historical transfers and process records (Herting et al. 1995). The major constituents include water, aluminum, chloride, chromium, hydroxide, nitrate, nitrite, phosphate, potassium, sodium, sulfate, total inorganic carbon and total organic carbon. The major radionuclides present in the waste are ^{137}Cs and ^{90}Sr . Prior to mixer pump operations, core sampling results and temperature profile measurements indicated the waste was composed of a crust floating on a liquid layer with a layer of settled solid material on the bottom (Babad et al. 1992). The liquid layer is referred to as the 'convective' layer because it is free to circulate in response to natural convection, and the solid layer is called the 'nonconvective' layer.

The historical tank estimate model (Jo 1997) predicts that AN-105 contains large amounts of sodium, aluminum, nitrite, nitrate, and hydroxide. The major radionuclides present in the waste are U, ^{137}Cs and ^{90}Sr (Jo 1997). Core sampling results and temperature profile measurements

indicate that the waste in Tank AN-105 has three distinct layers, similar to the waste in SY-101: the crust, convective layer, and nonconvective layer. Table 2.1 compares the waste present in SY-101 prior with mixer pump operations to the waste in AN-105 (Meyer et al. 1997). The nonconvective layer yield stress and viscosity values are calculated averages from ball rheometer measurements. Both the yield stress and viscosity of the nonconvective layer increase with the depth in the tank due to waste compaction under increasingly higher lithostatic pressures. As Table 2.1 shows, the physical properties of the waste in AN-105 are similar to the waste that was present in SY-101 prior to mitigation.

The next objective is to compare the waste gas composition of the two tanks. This comparison is presented in Table 2.2. The waste gas compositions in SY-101 prior to mixing were derived from the headspace gas composition following large gas releases (Sullivan 1995). The waste gas compositions in AN-105 were measured with the retained gas sampler (RGS) (Shekarriz et al. 1997).

Table 2.1. Physical Properties of SY-101 and AN-105 Waste

	SY-101 (prior to mitigation)	AN-105
Crust Thickness	122 cm (4 ft)	30 cm (1 ft)
Convective Layer (CL) Thickness	427 cm (14 ft)	549 cm (18 ft)
Nonconvective Layer (NC) Thickness	488 cm (16 ft)	457 cm (15 ft)
CL Density	1500 kg/m ³	1430 kg/m ³
NC Density	1700 kg/m ³	1590 kg/m ³
NC Yield Stress	≈225 Pa	≈130 Pa
NC Viscosity	≈20,000 Pa-s	≈12,000 Pa-s

Table 2.2. Waste Gas Composition in Tanks SY-101 and AN-105

	SY-101 (prior to mitigation)	AN-105
Ammonia (%)	6 ± 4	0.03 ± 0.03
Nitrogen (%)	35 ± 9	25 ± 2
Hydrogen (%)	30 ± 3	63 ± 4
Nitrous Oxide (%)	26 ± 2	11 ± 1
Methane (%)	0.37 ± 0.2	0.7 ± 0.1
Other Gases (%)	2.6 ± 0.4	0.3 ± 2
Diss. Ammonia (µm/L)	200,000	1400 ± 500

Meyer and coworkers (1997) calculated what the mixture concentrations in the tank headspaces would be at the LFL based on the compositions presented in Table 2.2. The volume of waste gas that would need to be released instantaneously to bring the headspace just to the LFL is then the product of the tank headspace volume and the calculated mixture LFL concentration. Dividing this volume by the total stored gas volume in the nonconvective layer gives the gas release fraction necessary to bring the tank headspace to the LFL. These headspace flammability values are presented in Table 2.3 for AN-105 waste and SY-101 waste prior to mixing. The nonconvective layer mean void fraction in SY-101 was not measured prior to mixing, so the void fraction was estimated based on void fraction instrument (VFI) measurements made after mitigation and the change in waste level. The total stored gas volume is the calculated volume of gas present at standard atmosphere and pressure based on the measured (or estimated) void fraction.

Table 2.3. Nonconvective Layer Flammability Summary for Tanks SY-101 and AN-105

	SY-101 (prior to mitigation)	AN-105
Nonconvective Layer Mean Void Fraction	8% (estimated)	4.2% (VFI measurement)
Nonconvective Layer Total Stored Gas Volume	394 ± 84 m ³	161 ± 30 m ³
Release Gas Volume To Reach LFL	125 ± 12 m ³	67 ± 4 m ³
Release Fraction To Reach LFL	0.30 ± 0.07	0.40 ± 0.08

Based on the data presented in Table 2.3, the maximum allowable instantaneous gas release from AN-105 during degassing to ensure that the 25% LFL limit is not exceeded is 25% of 67 m³, or 16.8 m³ (590 ft³). The maximum waste volume that can be disturbed at any one time is estimated to be 16.8 m³/161 m³, or 10% of the total waste volume, 185 m³ (6,532 ft³). Using this same procedure, the maximum allowable instantaneous gas release from Tank SY-101 during mixer pump operations would have been 31 m³ (1103 ft³).^(a) As was shown in Figure 2.2, the maximum cumulative gas release from SY-101 in a single day during Phase B testing was only 14.3 m³ (508 ft³) and the peak headspace hydrogen concentration was less than 2,500 ppm, much less than 25% of the LFL. The maximum cumulative gas release volume from SY-101 occurred early in Phase B testing, when the pump was first directed into the undisturbed waste. The AN-105 degassing strategy was based on this cumulative gas release data and is presented in Section 2.4.

2.3 Comparison of SY-101 and W-211 Pump Designs

As previously stated, the mixer pump used for SY-101 mitigation was originally purchased as a spare pump for the Hanford Grout program. The 112-kW (150-hp) pump was designed to operate between 100 and 1,180 revolutions per minute (rpm) and discharge a maximum 0.18 m³/s (2,800 gpm) of clear water through two opposed 6.6-cm (2.6-in.)-diameter nozzles. The pump

(a) The mixer pump safety analysis does not specify such a limiting release volume but prescribes a maximum headspace hydrogen concentration of 7,500 ppm (Sullivan 1995).

was modified for mitigation testing by extending the original discharge nozzles to keep the pump suction in the convective layer at an elevation of 6.6 m (260 in.), while allowing the nozzles to discharge into the nonconvective layer 71 cm (28 in.) above the tank bottom. The mixer pump was installed 0.9 m (3 ft) west of the tank center in riser 12A (Allemann et al. 1994).

Two 224-kW (300-hp) W-211 mixer pumps are proposed for use during AN-105 retrieval. The W-211 pumps are each designed to operate between 700 and 1,200 rpm and discharge a maximum 0.69 m³/s (11,000 gpm) of clear water through two opposed 15.2-cm (6-in.)-diameter nozzles. The inlet nozzles of each pump are located 17.8 cm (7 in.) above the tank bottom and the discharge nozzles are also in the nonconvective layer, 45.7 cm (18 in.) above the tank bottom. The two W-211 pumps will be installed 6.1 m (20 ft) north and southeast of the tank center in risers 007 and 008. Table 2.4 summarizes the design parameters for the SY-101 mixer pump and the W-211 pumps proposed for use during AN-105 waste retrieval. Figure 2.3 shows a schematic of the two mixer pumps.

Table 2.4. Design Parameters of the SY-101 and W-211 Mixing Pumps

	SY-101	W-211 (each pump)
Power	112 kW (150 hp)	224 kW (300 hp)
Speed	100 to 1,180 rpm	700 to 1,200 rpm
Pumping Capacity	0.18 m ³ /s (2,800 gpm)	0.69 m ³ /s (11,000 gpm)
Inlet Nozzle Location	6.6 m (260 in.) above tank bottom	17.8 cm (7 in.) above tank bottom
Discharge Nozzle Location	71 cm (28 in.) above tank bottom	45.7 cm (18 in.) above tank bottom
Discharge Nozzle Diameter	6.6 cm (2.6 in.)	15.2 cm (6 in.)
Tank Position	0.9 m (3 ft) west of tank center	6.1 m (20 ft) north and south-east of tank center (two pumps)

As is evident from Table 2.4 and Figure 2.3, the W-211 pumps proposed for use in Tank AN-105 are larger and more powerful than the SY-101 pump. The other main difference between the two pumps is that the intake of the SY-101 pump was located in the convective layer while the intake of the two W-211 pumps will be located in the nonconvective layer.

Since the mixer pump nozzles of the W-211 pump are very near the tank bottom, there is a concern that the initial action of the jets in the existing nonconvective layer will form a cavern or tunnel that does not penetrate into the nonconvective liquid layer. There is thus a potential for gas freed from the mobilized waste to collect in a pocket on top of the tunnel. If a subsequent pump run penetrated the roof of the tunnel, this gas volume would be released suddenly to the tank headspace along with any additional gas freed during the run—and might create a flammability hazard.

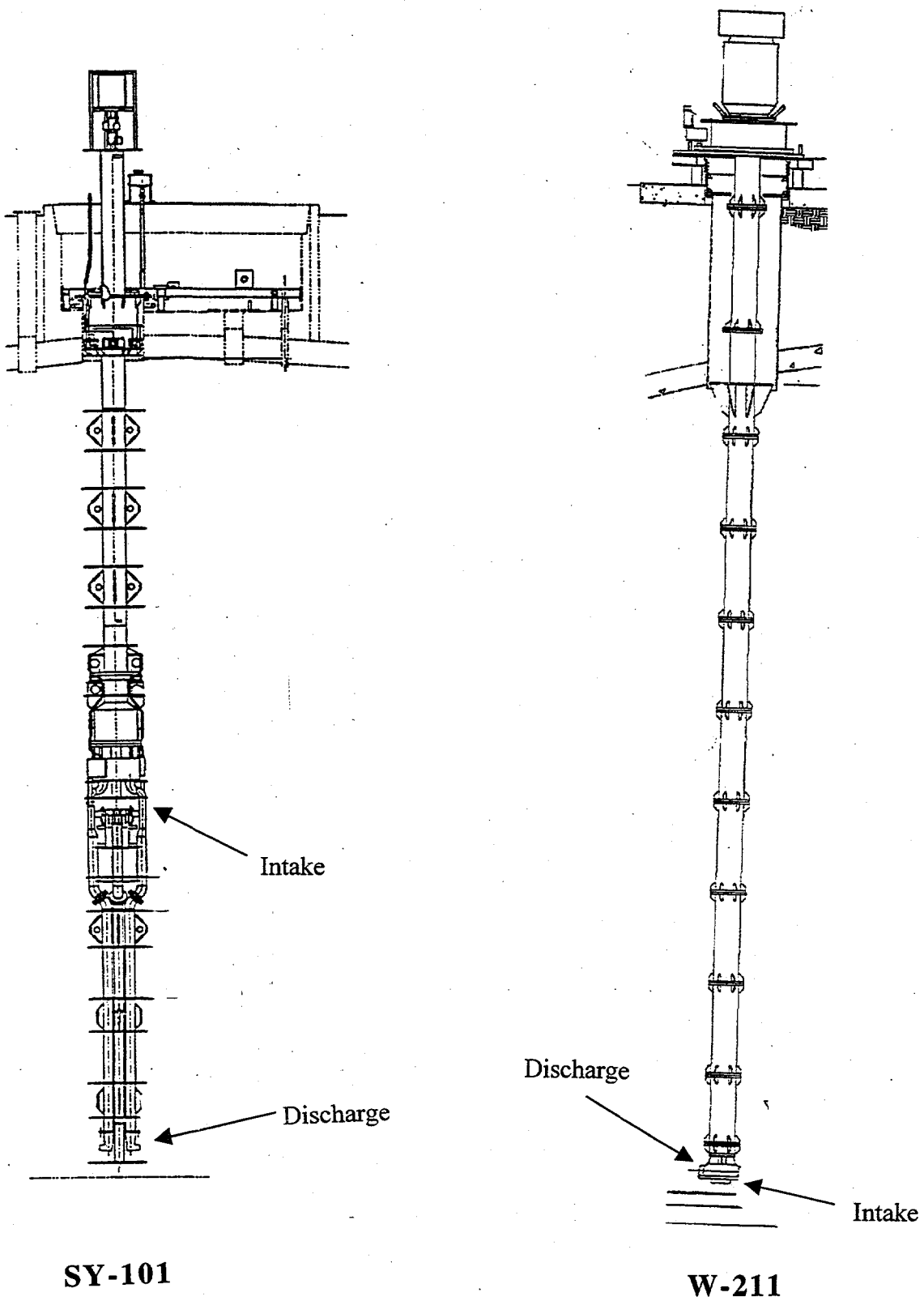


Figure 2.3. Schematic of the SY-101 and W-211 Mixer Pumps

However, the low strength of the waste makes tunneling unlikely, and, even if tunneling were to occur, the waste would be unable to retain a large bubble or dome of gas. The yield stress in the nonconvective layer in AN-105 increases linearly from essentially zero at the top to about 200 Pa near the bottom (Meyer et al. 1997). If the jet is able to penetrate the stronger lower region for any distance, it would more likely to follow the path of least resistance and excavate upward into the progressively weaker material rather than continue outward into the stronger material to form a tunnel.

If a tunnel were formed, the largest bubble or group of bubbles that could be retained is only the order of a few centimeters, far too little volume to be of concern. The limiting diameter of a spherical bubble in a Bingham fluid is expressed as (Chhabra and Uhlherr 1986):

$$D_{\max} = \frac{\tau_y}{\rho_w g Y_g} \quad (2.1)$$

where τ_y is the yield stress, ρ_w is the nonconvective waste density, g is gravitational acceleration, and Y_g is the "gravity-yield number," which is 0.2 for static or near-static conditions. The maximum diameter from Eq. (2.1) is plotted as a function of the yield stress in Figure 2.4. A material with yield stress of 200 Pa, the highest measured in AN-105, would be able to hold a spherical bubble of just under 5 cm

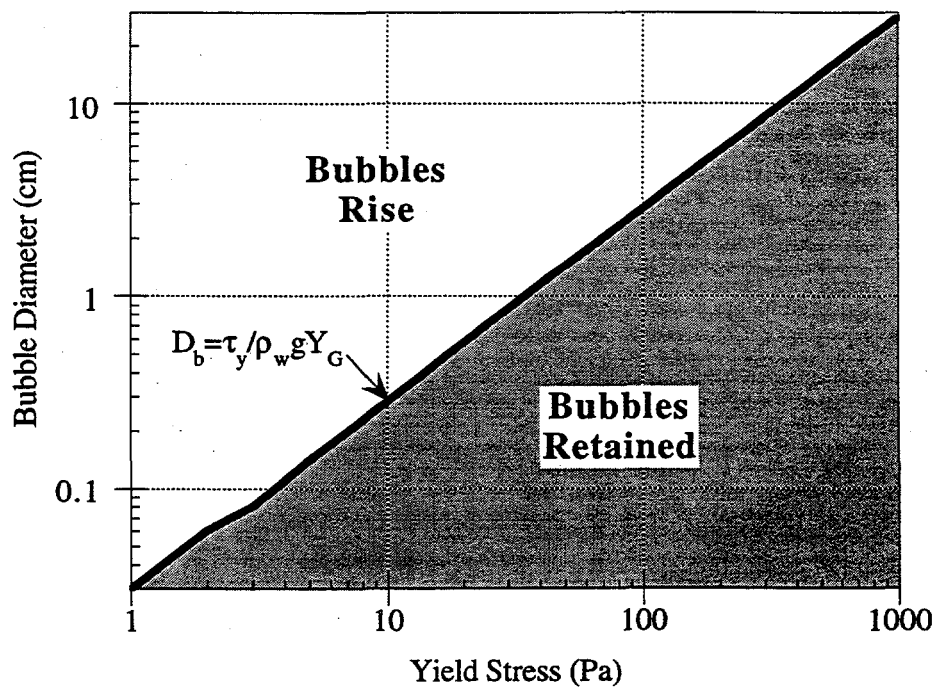


Figure 2.4. Maximum Retained Bubble Diameter versus Yield Stress

Though a bubble as large as 5 cm would not be expected to be spherical, Eq. (2.1) also specifies the maximum vertical extent of a bubble (based on the maximum difference in hydrostatic pressure the waste can withstand). Thus a gas layer on the roof of a tunnel would be limited to a maximum of 5 cm thick. A cylindrical tunnel roof 2 m in diameter (half the depth of the nonconvective layer) and 20 m in length would trap 0.4 m³ (14 ft³) of gas in a 5-cm layer. This is a very minimal gas release. However, the tunnel roof would have to be covered in waste with 2/3 to 1/2 the maximum strength. Therefore, it is more probable that a gas layer of only 2.5-3 cm (~1-in.) would be possible, cutting the potential gas volume by half. Tunneling cannot be seriously considered as a safety issue in AN-105.

Figures 2.5 and 2.6 show the plan views of Tanks SY-101 and AN-105, respectively. The locations of the mixer pumps and other important risers are identified in the figures. In SY-101, the mixer pump is located 0.9 m (3 ft) west of the tank center in riser 12A. Three risers contain waste surface level measuring instruments: 1A (located 6 m [20 ft] south of the tank center), 1C (located 6.2 m [20.2 ft] northeast of the tank center), and 17A (located 8.5 m [28 ft] southwest of the tank center). The waste level data shown in Figures 2.1 and 2.2 were from an FIC (Food Instrument Corporation) gauge in riser 1C.^(a) Temperature profiles are measured by thermocouples in the multifunction instrument trees (MITs) in risers 17B (located 8.5 m [28 ft] north of the tank center) and 17C (8.5 m [28 ft] southeast of tank center). VFI and ball rheometer (BR) tests were conducted in riser 4A (6.2 m [20.2 ft] southeast of tank center) in January and March of 1995, respectively (Stewart et al. 1996). In riser 11B, (8.5 m [28 ft] southeast of the tank center), VFI and BR tests were conducted in December 1994 and April 1995, respectively (Stewart et al. 1996). Additional VFI and BR tests are scheduled to be conducted in risers 1C and 11B in 1998.^(b)

In Tank AN-105, the risers have been given new identification numbers for retrieval purposes. Figure 2.6 reflects these new numbers. The two mixer pumps will be located 6.1 m (20 ft) north and southeast of the tank center in risers 007 and 008 (formerly 5B and 5A). Two risers, 002 (formerly 1A) (6 m [20 ft] west of the tank center) and 004 (2A) (6 m [20 ft] southeast of the tank center), are used to measure the waste surface level. One MIT will be relocated to riser 013 (2.7 m [9 ft] north of the tank center), which used to be known as riser 12A. RGS measurements were performed in June of 1996 on cores taken from this riser (Shekarriz et al. 1997). RGS measurements were also performed in June 1996 on samples from riser 009 (formerly 7B), which is located 6 m (20 ft) southwest of the tank center (Shekarriz et al. 1997). VFI and BR tests were conducted in risers 003 (6 m [20 ft] northeast of the tank center) and 018 (8.5 m [28 ft] east of the tank center) in December of 1995 (Stewart et al. 1996). These risers were previously numbered 1B and 16B, respectively.

The next step is to compare the projected performance of the two W-211 pumps proposed for use during AN-105 waste retrieval to the performance of the SY-101 pump during Phase B pump operations. Various pump parameters were monitored during SY-101 Phase B tests to observe and analyze pump operation. These included the average pump operating current and voltage and the average pump volute and nozzle pressure at the exit. Additional performance indicators were calculated from these measured quantities, including pump flowrate, motor input power, flow

(a) This FIC was replaced with an Enraf buoyancy gauge in 1995.

(b) Stewart CW. August 26, 1998. Personal communication. Pacific Northwest National Laboratory, Richland, Washington.

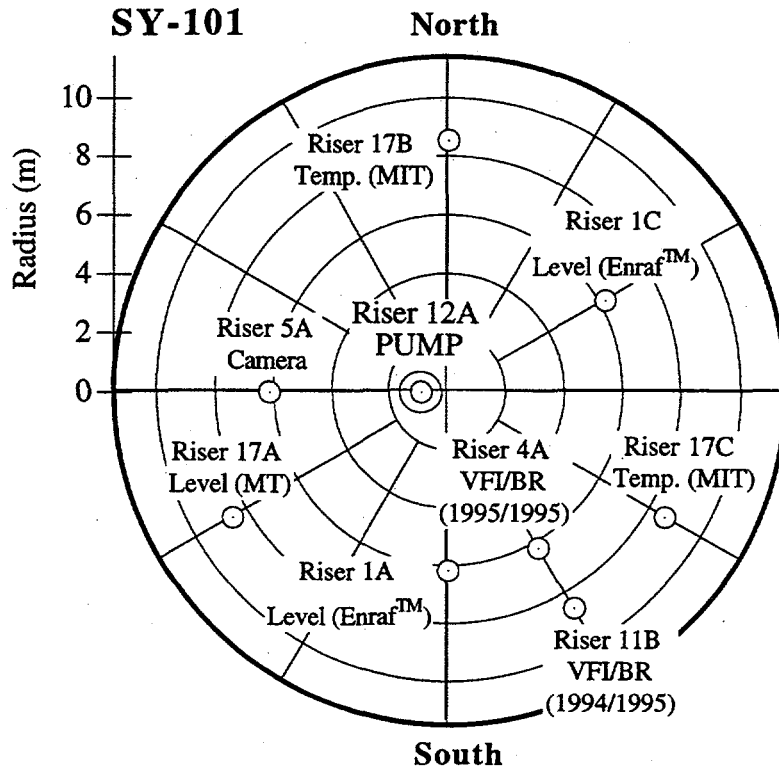


Figure 2.5. Plan View of Tank SY-101

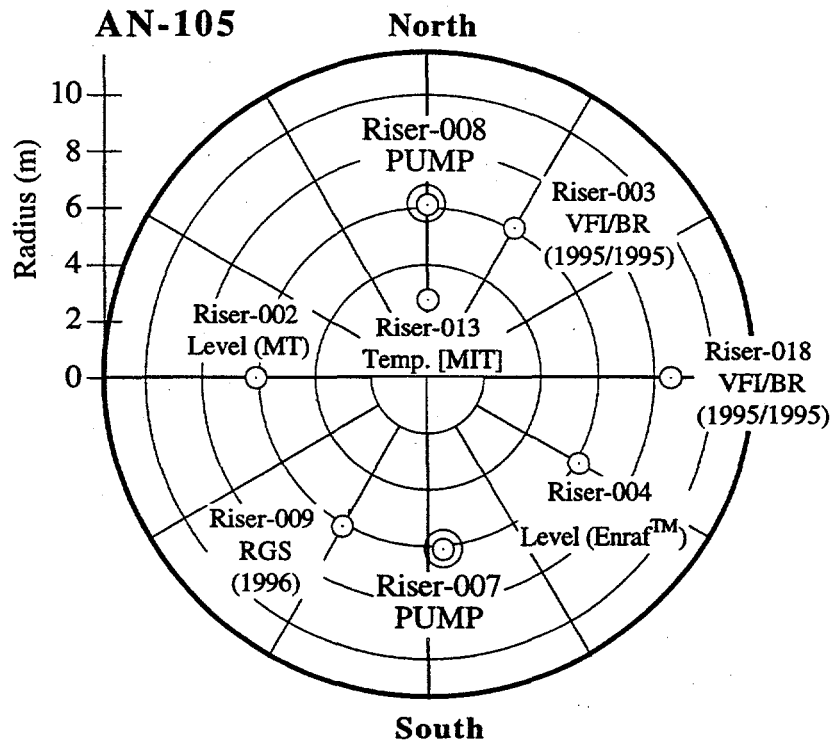


Figure 2.6. Plan View of Tank AN-105

(output) power, and efficiency (Allemann et al. 1994). The calculated pump flowrate as a function of pump speed during Phase B tests was used to calculate the jet velocity as a function of pump speed; the jet velocity per nozzle is equal to the pump flowrate divided by twice the area of the nozzle (because there are two nozzles per pump).

Figure 2.7 compares the parameter $U_o D$ (jet velocity times nozzle diameter) as a function of pump speed for the SY-101 pump and the W-211 pump. The parameter $U_o D$ is typically used in scaling and comparing pumps used for tank mixing. The jet velocity as a function of pump speed for the W-211 pump was calculated from the pump flowrate versus pump speed performance curve provided by the pump manufacturer, Lawrence Pumps, Inc. As is evident from Figure 2.7, the parameter $U_o D$ is larger for the W-211 pump than the SY-101 pump at equivalent pump speeds. In fact, at the minimum operating speed of the W-211 pump (700 rpm), the parameter $U_o D$ is larger than that of the SY-101 pump at its maximum operating speed of 1,000 rpm.^(a)

The pump flow power, output power, or hydraulic horsepower, defined as the rate of energy supplied by the pump to the waste, is shown in Figure 2.8 as a function of pump speed for both the SY-101 pump and the W-211 pump. The flow power was calculated for each pump per Equation (2.2), where ρ_s is the slurry density, Q is the pump flowrate, and U_o is the jet velocity.

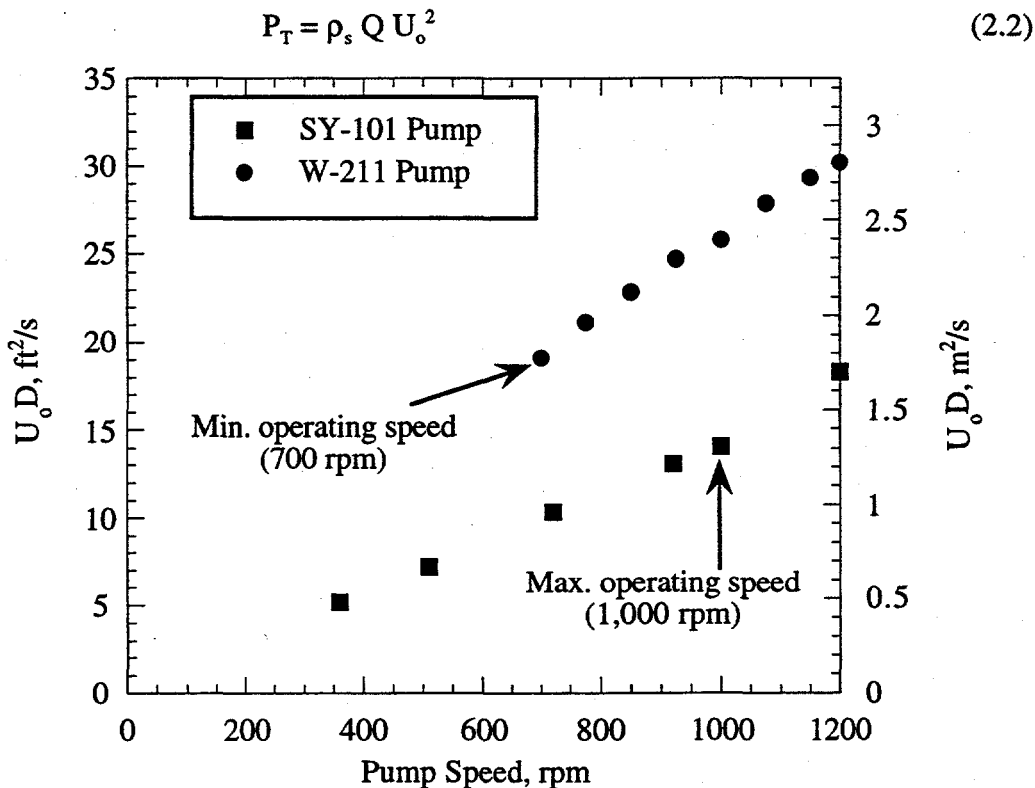


Figure 2.7. Comparison of SY-101 and W-211 Mixer Pump Performance

(a) The SY-101 pump can theoretically operate up to 1,180 rpm, but motor oil temperature limits reduce operating times at this speed to a few minutes. A 25-minute run is possible at 1,000 rpm.

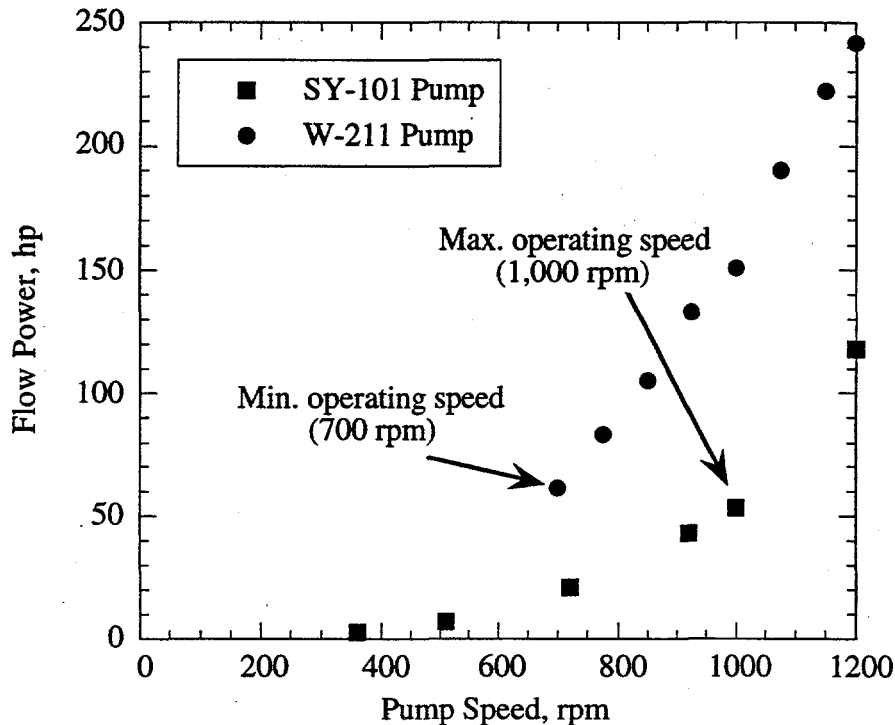


Figure 2.8. Pump Flow Power versus Pump Speed for SY-101 and W-211 Mixer Pumps

As shown in Figure 2.8, the flow power of the W-211 pump at its minimum operating speed of 700 rpm is slightly more than that of the SY-101 pump at its maximum operating speed of 1,000 rpm. Thus it is clear from Figures 2.7 and 2.8 that the W-211 pump is more powerful than the SY-101 pump. Because the SY-101 pump was successful at removing the bulk of the stored gas from SY-101 during Phase B testing, and because there will be two W-211 pumps in AN-105, each more powerful than the single SY-101 pump, it is concluded that the W-211 pumps will be successful at degassing Tank AN-105. In fact, the main concern is that the powerful pumps will mobilize the waste too quickly—and several constraints are imposed to prevent this. Section 2.4 presents the degassing strategy for Tank AN-105.

2.4 AN-105 Degassing Strategy

Because mitigation of SY-101 during phase B pump operations was successful, it is reasonable to base the degassing of AN-105 on these data. As discussed in Section 2.2, the maximum allowable instantaneous gas release from AN-105 during degassing was estimated to be 16.8 m³ (590 ft³). This value represents 25% of the volume of gas that would bring the headspace of AN-105 just to the LFL (Table 2.3). The maximum nonconvective layer volume that can be disturbed at any one time in Tank AN-105 and that can potentially release this amount of gas is estimated to be 10% of the total nonconvective layer volume, or 185 m³ (6,532 ft³). These values (the maximum allowable instantaneous gas release and mobilized nonconvective layer volume) represent the limiting conditions for degassing AN-105 and the monitoring and control strategy will need to ensure that they are not exceeded.

A challenge arises in attempting to predict which pump operation will disturb which nonconvective layer volume in AN-105 because there are no data or theory on which to base this prediction. We do not know how fast or how long the W-211 pump(s) can be run before the limiting volume of 10% of the nonconvective layer is mobilized. Over the past 10 years, PNNL has expended much effort in attempting to understand the physics of jet mixing in rheologically complex mixtures and applying this understanding to provide a better prediction of the mixing process in DSTs. These studies were aimed primarily at mobilizing and retrieving settled solids. The figure of merit for mixing performance is the effective cleaning radius (ECR), the radius measured from the pump centerline within which all the solids were suspended (i.e., "cleaning" the tank bottom). While the ECR may be a good measure of the ability of a jet to mobilize and suspend settled solids, effective degassing does not require total mobilization. It is only necessary to yield the waste so that trapped bubbles can escape by their own buoyancy. Nevertheless, we must make sure that any degassing strategy is conceptually consistent with the predicted ECR. Available ECR correlations are evaluated for the W-211 pump in the following paragraphs.

Data from 1/12-scale, 1/25-scale, and 1/50-scale jet mixing tests that were performed at PNNL between 1988 and 1997 were reduced using only dimensionless parameters and then curve-fitted to obtain correlations for the steady-state ECR of any given mixer pump in any given waste mixture (Equation 2.3) and the amount of time required to achieve this steady-state condition within the waste (Equation 2.4).^(a) The dimensionless parameters used in these correlations are

$ECR/D \equiv$ dimensionless effective cleaning radius

$\tau_s^* \equiv$ dimensionless shear strength or plasticity number $= \tau_s / \rho_s U_o^2$

$Re \equiv$ Reynolds number $= \rho_s U_o D / \mu_s$

$Fr \equiv$ Froude Number $= U_o / [(\rho_s - \rho) g D / \rho_0]^{1/2}$,

where: D (m) is the nozzle diameter, τ_s (N/m²) is the nonconvective layer shear strength, ρ_s (kg/m³) is the slurry density, U_o (m/s) is the nozzle exit velocity, μ_s (N-s/m²) is the slurry viscosity, ρ (kg/m³) is the density of water, g (m/s²) is gravitational acceleration, and ρ_0 (kg/m³) is the supernatant liquid density.

A standard multilinear regression analysis was used to correlate these parameters and obtain the best fit for the steady-state ECR:

$$ECR/D = 0.91 \tau_s^{*-0.17} Re^{0.2} Fr^{0.2} \quad (2.3)$$

The best-fit correlation for the amount of time required to achieve this steady-state condition within a tank is as follows, where D_t (m) is the tank diameter, h_c (m) is the convective layer thickness, and h_{nc} (m) is the nonconvective layer thickness:

$$t \text{ (seconds)} = \left[\left(\frac{D_t}{D} \right)^2 \frac{h_c}{4U_o} + 2 \left(\frac{ECR}{D} \right)^2 \frac{h_{nc}}{U_o} \right] \quad (2.4)$$

(a) Shekarriz A, JN Chung, CT Crowe, and D Sprecher. 1998. Letter report, "Physics of Jet Mixing in Rheologically Complex Mixtures," Pacific Northwest National Laboratory, Richland, Washington.

The problem with using Equations (2.3) and (2.4) to predict steady-state conditions during degassing is that during the 1/12-scale, 1/25-scale, and 1/50-scale jet mixing tests, the pump was continuously rotated at 0.5 rotations per minute, while during degassing the pump nozzle orientation will be fixed for a designated period of time and then rotated. Because the only "real" data available on jet mixing in actual DST waste are from SY-101 mitigation, the AN-105 degassing pump run time was based on these data. The correlations in Equations (2.3) and (2.4) were used to substantiate the selected degassing pump run time.

As presented in Section 2.3, the minimum operating speed of the W-211 pump is 700 rpm (60% speed) and the pump flow power (rate of energy supplied by the pump to the waste) at this speed is slightly greater than the pump flow power of the SY-101 pump at 1,000 rpm. To ensure that pump operations do not release more than the allowable instantaneous gas volume of 16.8 m³ (590 ft³), the W-211 pumps in AN-105 must be operated one at a time, in a fixed direction and at their minimum operating speed of 700 rpm for a limited time.

The W-211 pump run times are based on the maximum gas release volume measured in Tank SY-101 as the pump was first directed into the undisturbed waste. As presented in Figure 2.2, the maximum cumulative gas release from SY-101 in a single day during Phase B testing was 14.3 m³ (508 ft³). This maximum daily gas release occurred on November 5, 1993 during Phase B test B-5. The pump nozzles were aimed at 65° and 245°, and the pump was run for 20 minutes at each of four speeds (360, 510, 720, and 920 rpm) for a total of 80 minutes. The calculated energy supplied by the pump to the waste during test B-5 was approximately 18.2 kW-hr (24.4 hp-hr). One of the W-211 pumps operating at 700 rpm would supply this same amount of energy to AN-105 waste in approximately 24 minutes. Subsequently, it has been suggested that during degassing each W-211 pump be run individually at 700 rpm for 24 minutes in varying directions in order to remove the bulk of the stored gas while ensuring that gas release rates remain less than the maximum allowable.

The validity of a 24-minute pump run was assessed against the steady-state ECR correlation presented above. Using Equations (2.3) and (2.4) and the AN-105 waste properties presented in Table 2.1 as well as the W-211 pump properties presented in Table 2.4, the estimated steady-state ECR is 7.6 m (25 ft) and the time to reach this steady-state condition is 80 minutes. The estimated effected nonconvective waste volume for an ECR of 7.6 m (25 ft) is 101 m³ (3,566 ft³), assuming only the waste within a 30° sector in opposing directions is mobilized. This volume is less than 10% of AN-105's nonconvective waste volume, which, as previously stated, is the maximum that can be mobilized at any one time. Based on these steady-state estimates, the proposed 24-minute pump run time during degassing of Tank AN-105 is apparently conservative and should ensure that gas release rates remain less than the maximum allowable. Another indication that the 24-minute pump run time is conservative is that it was based on the maximum cumulative release of gas from SY-101 rather than on average or instantaneous values. A proposed degassing schedule and monitoring and control strategy are presented below.

As discussed, it has been proposed that during the degassing of Tank AN-105 each W-211 pump be run individually at 700 rpm for 24 minutes in fixed directions at 45° increments to remove the bulk of the stored gas while ensuring that gas release rates remain less than the maximum allowable. Figure 2.9 shows the proposed pump operation schedule along with the nozzle orientations. Because each pump has two opposing nozzles, a 0° orientation also directs a jet at 180°. The pump in riser 008 will be used during the first pump run with the nozzles N-S at 0-180 degrees. The second pump run will use the pump in riser 007, also with its nozzles N-S at 0-180 degrees. Subsequent runs will alternate pump use and vary the nozzle directions. Each pump run will last 24 minutes with a minimum one-day waiting time between runs to ensure that

any delayed gas releases occur before the next run. The one-day wait time is based on SY-101 mitigation experience. A complete tank sweep using both pumps should be accomplished in a minimum of eight days, assuming there are no alarms causing pump operation to be aborted or other delays due to weather, etc.

The arrows in Figure 2.9 represent the effective degassing radius (EDR). There is no mixing theory or data to indicate what this degassing radius will be after 24 minutes of pump operation. As presented earlier, the estimated steady-state ECR is 7.6 m (25 ft), however, it was calculated with a correlation derived from scaled, jet mixing-tests where the pump was continuously rotated, so it may not represent a true steady-state condition for pump operation during degassing.

However, the progress of jet penetration during AN-105 mixing can be monitored during the first pump run by observing the temperature on the bottom four thermocouples on the MIT in riser 013. Riser 013 is 3.4 m (11 ft) south of pump 1 (riser 008). By observing changes in the temperature profiles in response to pump operation, it is possible to infer how and if pumping has transformed the waste in the vicinity of riser 013. An example of how these temperature data can be used to determine jet penetration is shown in Figure 2.10. The temperature trends for SY-101's riser 17B MIT thermocouples 1, 2, 3, and 4 (the lower four thermocouples) are shown right before and after a full-scale jet penetration test (Stewart et al. 1994). These temperature trends show

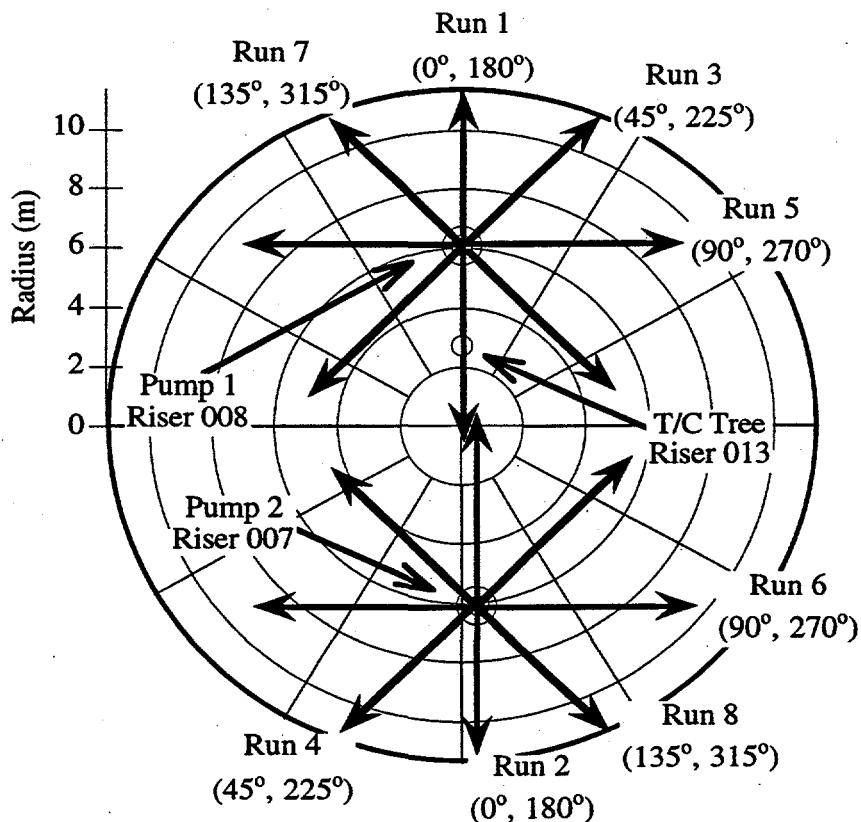


Figure 2.9. Proposed Pump Run Schedule for AN-105 Degassing

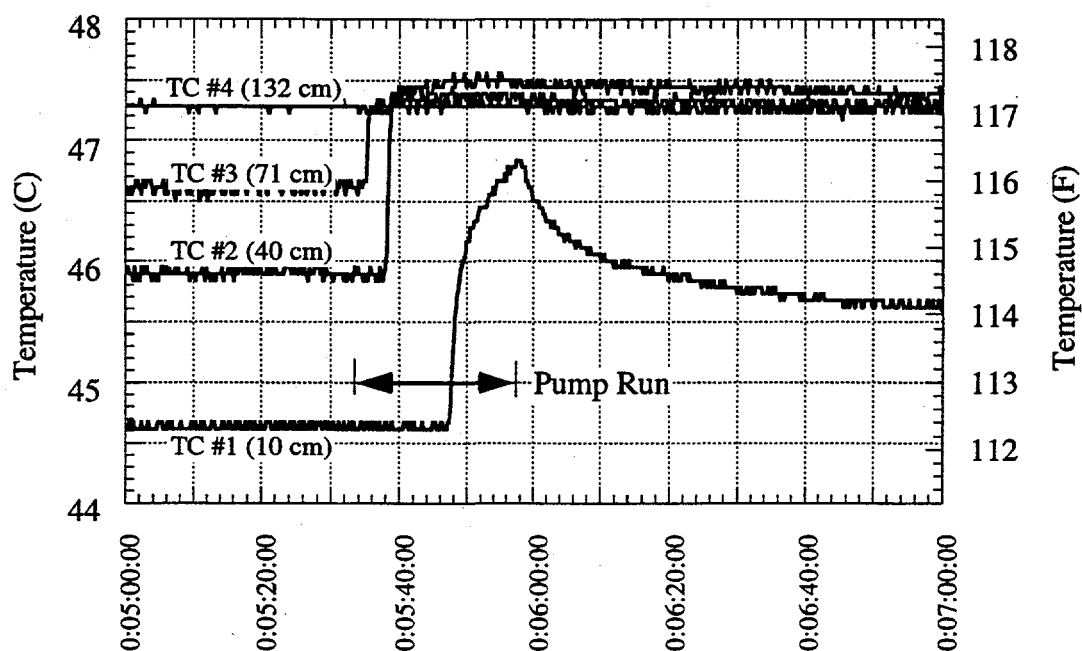


Figure 2.10. Temperature Trends at Riser 17B During a SY-101 Jet Penetration Test

direct evidence of sludge excavation by the jet. Thermocouples 2 and 3 (40 cm and 71 cm above the tank bottom, respectively) responded almost immediately to the jet and, even after the pump was turned off, the temperatures remained high, indicating that the waste at these levels had become convective. The lowest thermocouple, at 10 cm (4 in.) above the tank bottom, took longer to respond, but within about 15 minutes of the start of the pump run the temperature increased almost 2°C, indicating that the jets did penetrate the sludge at this level.

After all eight pump runs have been completed, a decision will be made whether to perform additional pump runs based on the cumulative amount of gas that was removed and an assessment of how much nonconvective waste was mobilized by the pumps. Gas chromatographs (GCs) measure hydrogen and other gases in the tank headspace; these concentrations can be multiplied by the ventilation flowrate and integrated over time to determine the cumulative amount of gas removed beyond the baseline or background release rate.

If it appears that a significant amount of stored gas still remains in the waste and/or that a large fraction of the nonconvective waste has not been mobilized, additional pump runs will be made. It is possible that the 24-minute pump run time could be increased or decreased depending on the results obtained during the first round of pump runs. Pump runs will continue until it has been determined that too little stored gas remains in AN-105 to permit continuous operation of both pumps without exceeding 25% LFL.

2.5 Monitoring and Control

The specific objective of running the W-211 pumps during AN-105 degassing is to remove as much gas from the waste as possible in a reasonably short period of time without exceeding the LFL in the tank headspace. This objective should be pursued subject to the controls presented below.

- Short-term pump operation should be controlled by conditions in the headspace, namely vent flow and gas composition (i.e., shut down if headspace approaches 25% LFL).
- Long-term pump operation should be controlled to prevent undesirable changes in the waste, namely excessive temperature or unexpected level change (e.g., foaming).

To monitor the gas releases in response to pump operation, it is necessary to measure the vent header flow rate, the concentration of hydrogen, nitrous oxide, and ammonia at the vent header, the temperature profile, and the waste surface level. The vent header flow rate in SY-101 was measured with an averaging pitot probe in the ventilation header at riser 7A. Combined with gas composition information, the ventilation volume flow rate yielded actual hydrogen, ammonia, and nitrous oxide release rates. The total gas release in SY-101 was obtained from the hydrogen release rates using data from gas samples to estimate the hydrogen fraction of the total released gas. Gas compositions in the vent header were determined by two GC systems that measured hydrogen concentration and a Fourier Transform Infrared Spectrometer (FTIR) that gave nitrous oxide and ammonia concentrations. During AN-105 degassing, it is recommended that the same procedure used during SY-101 mitigation be employed for measuring gas releases in AN-105. The vent header flow rate and the gas compositions in the vent header should be recorded automatically at least hourly to make full use of the information provided.

Because the waste generates heat, the highest quality and greatest amount of information on the changes induced in the waste by mixing are obtained from waste temperature measurements. In SY-101, waste temperatures were obtained from the 22 thermocouples on the MITs in risers 17B and 17C. During AN-105 degassing, it is recommended that the MIT in riser 013 be used to measure the waste temperatures throughout the waste depth and that these data be recorded automatically at least hourly to make full use of the information provided.

The waste surface level is the only available direct indicator of total gas content in the waste. As gas accumulates, the surface level rises; as gas is released, the surface level decreases. The surface level also varies with changing atmospheric pressure in proportion to the amount of gas contained and its depth. Unfortunately, measuring a tank's surface level is difficult because it is very rough and irregular. In SY-101, four different instruments were employed to measure waste level: a manual tape in riser 17A, an FIC contact probe in 1C, an Enraf-Nonius radar gauge in 13A, and an Enraf buoyancy gauge in 1A. The FIC became unreliable and was replaced by a second Enraf gauge in 1995. The radar gauge became essentially inoperative in 1995, probably because of radiation damage. The Enraf buoyancy gauge in riser 1A was the most accurate and reliable, and in 1995 was connected directly to the Data Acquisition System (DACS) system for automated readings. During AN-105 mixing, an Enraf buoyancy gauge is recommended for waste level measurements. These data should be recorded automatically at least hourly to make full use of the information provided.

3.0 Dissolved Gas Release

The first phase of waste retrieval for AN-105 involves thoroughly mixing the tank contents with mixer pumps, allowing the solids to settle out, and then pumping all of the liquid out of the tank. The liquid will be diluted with a water/caustic diluent and pumped into intermediate feed staging tanks (IFSTs). Existing DSTs AP-102 and AP-104 have been proposed as possible IFSTs for this process. Once the solids have resettled in AN-105, dilution water/caustic will be added to the remaining slurry and mixed with the mixer pumps to dissolve the maximum amount of solids. One question that must be answered before proceeding is how the dissolved gas (mainly ammonia) released during these processes will affect the flammability in AN-105 and the IFST(s).

The dissolved gas release modeling approach developed in Peurrung et al. (1998) for analysis of the double-contained receiver tanks (DCRTs) can be used to address this question, since it is in many respects the same problem. Peurrung and coworkers (1998) developed two models: the "equilibrium" and "nonequilibrium" models. The equilibrium model conservatively assumes that there is unlimited mass transfer between the liquid and gas, so that dissolved gases are in equilibrium with the vapor. In the nonequilibrium model, dissolved gases are modeled as volatilizing from the falling inlet stream and the standing liquid surface such that mass transfer may not permit the vapor to reach equilibrium with the liquid.

Both models assume that gas is carried only in solution, with "hitchhiker" bubbles and gas adsorbed on carryover particles being negligible. Vapor-liquid equilibrium is represented by Henry's Law, with solubilities calculated using the Schumpe model and parameters that were experimentally tested and reported in Norton and Pederson (1995). The headspace in each tank is assumed to be well mixed. Thermal, radiolytic, and corrosion-produced hydrogen generation in the waste in AP-102 and AP-104 was modeled according to the algorithm presented in Hu (1997). The assumptions used in the DCRT models apply equally well to the transfer between AN-105 and AP-102/AP-104. (Refer to Peurrung et al. (1998) for complete documentation of the analytical models, including discussion of limiting assumptions, validation against other models, and range of applicability.)

Calculations were performed for the proposed transfer of liquid from AN-105 to AP-102. Two cases were considered:

Case 1 -- 1,890 kL (500 kgal) of undiluted supernatant from AN-105 is transferred to AP-102; this represents the initial transfer of existing liquid and potentially represents the highest headspace flammability in the receiver tank.

Case 2 -- 3,822 kL (1,011 kgal) of waste resulting from 80% dilution of settled solids with water is mixed in AN-105; this case explores the extent to which dilution and the absence of a crust affects the headspace flammability in the source tank.

3.1 Input Parameters and Boundary Conditions

The current conditions in AN-105 were selected as the baseline for these calculations. The receiver tank, AP-102 or AP-104, was assumed to have geometry identical to AN-105, with the following relevant dimensions:

- total volume: 5,314 m³ (187,624 ft³)
- tank diameter: 22.9 m (75.15 ft)
- tank cross-sectional area: 412 m² (4434.77 ft²).

The current contents of AN-105 are reported as follows (Meyer et al. 1997; Hanlon 1998):

- crust thickness: 0.3 m (0.98 ft)
- convective layer depth: 5.59 m (18.34 ft)
- nonconvective layer depth: 4.52 m (14.83 ft)
- total volume of waste: 4,283 kL (1,133 kgal)
- volume of supernatant: 2,298 kL (608 kgal).

The inlet port for the fluid being transferred into AP-102 is expected to be a 10.2-cm (4-in.) inside diameter (i.d.) riser, vertically oriented, terminating about 14 m (46 ft) above the bottom of the tank. Assuming the tank initially contains a 15.2-cm (6-in.) heel, the height of the injection port means that the maximum distance the liquid can fall upon entering the receiver tank is 13.85 m (45.5 ft). If a total of 1,890 kL (500 kgal) of liquid is transferred from AN-105, the maximum depth of the liquid in Tank AP-102 is 4.75 m (15.57 ft). The final filled volume fraction for the receiver tank in Case 1 is 0.344, including the initial heel.

Case 2 assumes that AN-105 is pumped down to 0.61 m (2 ft) of supernatant, leaving only enough liquid for the suction of the pump. At this level, 1,984 kL (525 kgal) of settled solids and 249 kL (66 kgal) of supernatant would remain. Enough diluent is assumed to be added to provide 80% dilution of the solids (which would require 1,588 kL (420 kgal) of diluent). This addition gives a total waste volume in AN-105 of 3,821 kL (1,011 kgal), counting diluent, solids, and remaining supernatant, and assuming no volume is lost as solids dissolve.

The values used in these calculations are listed in Table 3.1. The "fill scenario" data (fill rate, final fraction of the tank filled, mixing rate, and ventilation rate) were obtained from cognizant Project Hanford Management Contract personnel.^(a) The input parameters to describe the density, salt concentrations, total organic carbon (TOC), and water concentrations of the liquid waste for the Case 1 undiluted supernatant were obtained from the Core 152 liquid composite reported in the AN-105 Tank Characterization Report (Jo 1997). For Case 2, those parameters were obtained from the Series V data reported in Herting (1997). Those data represent 80% dilution with water of the settled solids from an AN-105 whole-tank composite sample.

(a) Rieck CA (Numatec Hanford Corporation). May 11, 1998. Personal communication to LA Mahoney, Pacific Northwest National Laboratory.

Table 3.1. Model Input Parameters

Input Parameter	Case 1: Undiluted Supernatant Transferred to AP-102	Case 2: 80% Dilution of Settled Solids with Water, Mixed in AN-105
Ventilation rate (acfm)	145	100
Fill rate (gpm)	140	0
Pump mixing rate (gpm)	0	20,720
Final fraction of tank filled	0.344	0.720
Conc. in the waste liquid (M):		
Na ⁺	10.78	9.77
AlO ₂ ⁻	1.54	1.06
Cr ³⁺	0.000468	0.022
K ⁺	0.01	0.15
OH ⁻	0.01	0.01
NO ₃ ⁻	2.62	2.20
NO ₂ ⁻	2.65	1.69
CO ₃ ⁻	0.31	0.31
PO ₄ ⁻	0.0123	0.068
SO ₄ ⁻	0.0298	0.22
F ⁻	0.0226	0.063
Cl ⁻	0.27	0.18
Waste liquid density (kg/m ³)	1420	1360
Waste pH	12	12
Mass fraction of water (wt%)	50.1%	64.3%
¹³⁷ Cs concentration (Ci/mL)	0.000475	0.000193
TOC concentration (g/L)	6.10	2.04
Waste temperature (°C)	46	46
Pressure in source tank (atm)	1.0	1.0
Source tank dissolved gases:		
NH ₃ concentration (M)	0.025	0.011
H ₂ mole fraction in gas	0.243	0.107
H ₂ concentration (M)	5.9 x 10 ⁻⁶	2.6 x 10 ⁻⁶
CH ₄ mole fraction in gas	0.013	0.0057
CH ₄ concentration (M)	1.9 x 10 ⁻⁷	0.86 x 10 ⁻⁷
Nonflammable mole fraction in gas	0.744	0.887
Nonflammable concentration (M)	6.1 x 10 ⁻⁶	7.4 x 10 ⁻⁶
Ratio of N ₂ /H ₂ in gas	0.744/0.243	0.887/0.107
Ratio of CH ₄ /H ₂ in gas	0.013/0.243	0.0057/0.107

Because the transfer procedure has not been fully determined yet, some input parameters represent reasonable estimates. These include the waste temperature (set at the maximum temperature currently measured in AN-105 waste) and the average gas pressure in the source tank (set at 1 atm to reflect the fact that mixing would keep the source liquid in equilibrium with the pressure at the surface). In Case 1, the mole fractions of hydrogen, methane, and nonflammable gas in the low-solubility retained gas (which are used to calculate the dissolved concentrations of these species) were calculated from the composition of the gas inventory retained in the AN-105 supernatant, as measured by RGS (Shekarriz et al. 1997).

The dissolved ammonia concentration in the undiluted AN-105 liquid is a dominant parameter in the headspace flammability calculation. Different values have been found for it in available reports. The lowest estimate, 0.0017 mol NH₃/L waste, was obtained from one interpretation of the RGS data (Shekarriz et al. 1997) and is regarded as an underestimate. This value corresponds to an ammonia concentration of about 0.0025 M in the liquid alone, based on the solid and gas volume fractions in this reference. The highest estimate is 0.104 M NH₃, based on another interpretation of RGS data (Kubic and Pillay 1997). This value is believed to be an overestimate. It is not supported by independent analysis of the ammonia that remained in the RGS samples after the gases and a small amount of ammonia vapor had been extracted.^(a)

The analytical measurements of the residual ammonia (which are recorded in the LABCORE database) were performed with ion-specific electrodes, after water digest of two of the RGS samples. They showed that the residual ammonia concentrations (those remaining in the samples after vapor extraction) were 9,588 mmole/L waste (segment 15) and 7,529 mmole/L waste (segment 18).^(b) It should be noted that the analytical measurements of residual ammonia might have been low because of ammonia evaporation during sample preparation and analysis. The upper limit for the ammonia loss under those circumstances has been estimated as half of the original sample ammonia (this amount of loss would probably require that the sample be exposed to air for about 2 hours).^(c) However, data indicate that the loss is only 30% for the more probable exposure time of half an hour; therefore the analytical values are multiplied by 1.5 to obtain a best estimate of the true value.

The amount of ammonia vapor that was extracted from the RGS samples was also underestimated in Shekarriz et al. (1997) because no account was taken of the ammonia dissolved in the water that condensed in the collector owing to compression during pumping. In Tanks U-103, S-106, and BY-109 (Mahoney et al. 1997), the dissolved ammonia in the collector was found to be roughly equal to the vapor-phase ammonia. Thus multiplying the values for extracted ammonia reported in Shekarriz et al. 1997 by a factor of 2 should result in a best estimate of the true extracted ammonia. The reported values were 1,106 mmole/L waste (segment 15) and 1,426 mmole/L waste (segment 18).

Multiplying the residual ammonia by 1.5 and the extracted value by 2 gives best-estimate total ammonia concentrations of 16,600 mmole/L waste (segment 15) and 14,100 mmole/L waste (segment 18). These concentrations in the total waste volume translate to 0.025 M NH₃ and 0.021

(a) Mahoney LA. 1998. "Preliminary Review of RGS Ammonia Measurement Methods." TWS98-58, Pacific Northwest National Laboratory, Richland, Washington.

(b) Samples S96R000422 and S96R000548. LABCORE database.

(c) Herting DL. October 7, 1994. "Rate of Ammonia Loss from Laboratory Samples." Letter report to GD Johnson, Westinghouse Hanford Company, Richland, Washington.

MNH₃ in the AN-105 liquid alone. A concentration of 0.025 M is therefore used as input for the dissolved ammonia in the undiluted liquid pumped from AN-105 to AP-102 in Case 1.

The Case 2 inputs for the dissolved ammonia, hydrogen, methane, and nonflammable gas are found from the dilution of the supernatant and interstitial liquid in AN-105. If it is assumed that the settled solid volume contains about 50 vol% interstitial liquid, a reasonable approximation can be obtained based on the relative densities of liquid, solids, and bulk waste. Then 1,588 kL (420 kgal) of diluent containing only nonflammable dissolved gases are added to 1,240 kL (328 kgal) of supernatant and interstitial liquid. As a result, the concentrations of dissolved flammable gases (as used in Case 1) are reduced by 56% in the liquid modeled in Case 2.

3.2 Results

The calculated concentrations of flammable gases predicted for the two cases using both the equilibrium and nonequilibrium models are summarized in Table 3.2. The calculated concentrations are also expressed in terms of the percent of the LFL for the particular gas. To ensure that ignition will not occur in a tank under any conceivable circumstance, the concentrations of flammable gases must be maintained at values corresponding to less than 25% of the LFL for the particular gas. As seen in Table 3.2, for both cases, the concentrations of the flammable gases are far below 25% of the LFL of the gas.

Both the equilibrium and nonequilibrium models predict that the flammable gas in the AP-102 headspace over the undiluted supernatant (Case 1) will be 4% to 4.5% of the LFL. The maximum flammability in the AP-102 headspace exists immediately after filling; thereafter the flammability decreases as ventilation slowly dilutes the headspace with air.

When the solids in AN-105 are 80% diluted (Case 2), these models predict that the flammable gas in the AN-105 headspace over the diluted waste will be approximately 1.6% of the LFL, which is less than half the value from Case 1.

In both cases, most of the flammable gas is ammonia. In Case 1, the concentration of ammonia corresponds to 3.9% to 4.4% of the LFL for ammonia. The concentration for hydrogen in this case corresponds to only about 0.1% of the LFL for hydrogen. In Case 2, the concentration of ammonia corresponds to about 1.5% of the LFL for ammonia, less than half of the value in Case 1. The concentration of hydrogen in AN-105 for Case 2, however, corresponds to about 0.1% of the LFL for hydrogen, the same value as for the undiluted waste in AP-102.

Table 3.2. AN-105 Flammability Analysis for Postulated Cases of Liquid Waste Transfer and Dilution

Calculated LFL Values	Case 1: Undiluted Supernatant Transferred to AP-102	Case 2: 80% Dilution of Settled Solids with Water, Mixed in AN-105
Equilibrium Model: Flammable gas concentrations: ammonia (ppm) hydrogen (ppm) methane (ppm)	6500 44 0.6	2300 39 1.4
Maximum % of LFL	4.5 % (at the end of fill) 4.4% (ammonia) 0.1% (hydrogen) 0.0% (methane)	1.6 % (total) 1.5% (ammonia) 0.1% (hydrogen) 0.0% (methane)
Steady state % of LFL after filling	0.1% (H ₂)	
Peak % of LFL	4.5%, decreases immediately after fill is complete	1.6%
Nonequilibrium Model: Flammable gas concentrations: ammonia (ppm) hydrogen (ppm) methane (ppm)	5900 17 0.5	2300 20 0.6
Maximum % of LFL	4.0 % (at the end of fill) 3.9% (ammonia) 0.0% (hydrogen) 0.001% (methane)	1.6% (total) 1.5% (ammonia) 0.0% (hydrogen) 0.001% (methane)
Steady state % of LFL after filling	0.1% (H ₂)	
Peak % of LFL	4.0%, decreases immediately after fill is completed	1.6%

4.0 Maximum Waste Temperatures

The objective of this analysis was to predict maximum waste temperatures for the variable waste layer depths, conditions, and compositions that might occur in AN-105 during retrieval operations. A two-dimensional thermal computer model of AN-105 was used to simulate two different waste retrieval scenarios. The first simulation was a transient run of a 180-day cooldown period for AN-105 after the waste had been fully mixed to a uniform consistency and pump power input had elevated the waste temperature. The second was a steady-state calculation of AN-105 after the supernatant layer was decanted. In this scenario, the only remaining waste in the tank was the original nonconvective layer.

Several factors determine the temperature distribution within a DST, including air flows through the primary tank and annulus regions, waste stratification and the depths of the strata, the thermal and physical properties of the waste, and the heat generation rate. AN-105 has a temperature profile similar to that observed in SY-101 prior to pump mixing. These profiles have isothermal and parabolic regions indicative of convective and nonconvective heat-generating layers, respectively. AN-105 may have had temperature profile changes following surface level drops that indicate the release of gas from a nonconvective layer (Reynolds 1994). The annulus vent air flow rate has varied in the recent past due to blower problems (Reynolds 1994) and the subsequent installation of a constant flow exhaust controller in 1995 (Wilkins et al. 1997).

4.1 Thermal Modeling Approach

These simulations were performed with the hydrothermal model in the TEMPEST code. TEMPEST numerical procedures are based on semi-implicit, finite-difference methods (Trent and Eyler 1997). These procedures can be used to solve time-dependent equations governing three-dimensional mass, momentum, and energy conservation for incompressible flows. Momentum equations are solved explicitly with implicit viscosity; the continuity and pressure solution is obtained implicitly. The solutions to scalar equations (energy, turbulence, constituent, electromotive force) are also obtained implicitly; energy transport and electromotive force are solved for both fluid and solid regions.

The approach chosen to analyze the waste temperatures within AN-105 was to implement a two-dimensional TEMPEST model developed for double-shell Tank SY-101.^(a) The model consists of 52 radial cells and 66 vertical cells with variable cell spacing. Fine cell spacing was used in regions of large thermal gradients and where thermal radiation was modeled. A constant temperature of 16°C (60°F) was maintained in the earth at the far vertical and radial boundaries.

The model was modified to represent the current waste configuration and air flow rates in AN-105. The model included heat transfer by conduction, convection, and radiation. Figure 4.1 represents a schematic of the domain under consideration. The waste was represented as three distinct layers: a crust, a convective liquid layer, and nonconvective waste, each with unique thermal and physical properties, as summarized in Table 4.1. Waste layer depths were estimated

(a) Antoniuk, Z. I. 1994. *Study of Tank 241-SY-101 Thermal Behavior Using the TEMPEST Code*. PNLMIT:030394, Pacific Northwest National Laboratory, Richland, Washington.

from thermocouple and ball rheometer data; these and measured waste properties were from Stewart et al. (1996). Heat capacities chosen for the waste within AN-105 were those reported for SY-101. Properties used for the tank structure and surrounding earth are listed in the lower portion of Table 4.1. Air was assumed to circulate in the dome above the crust, in channels below the tank inner shell, and between the tank annulus shells. Heat transfer with the annulus air inflow tubes was neglected as in earlier SY-101 analyses; the air was assumed to enter the bottom channels at the same temperature as the prescribed dome air inlet.

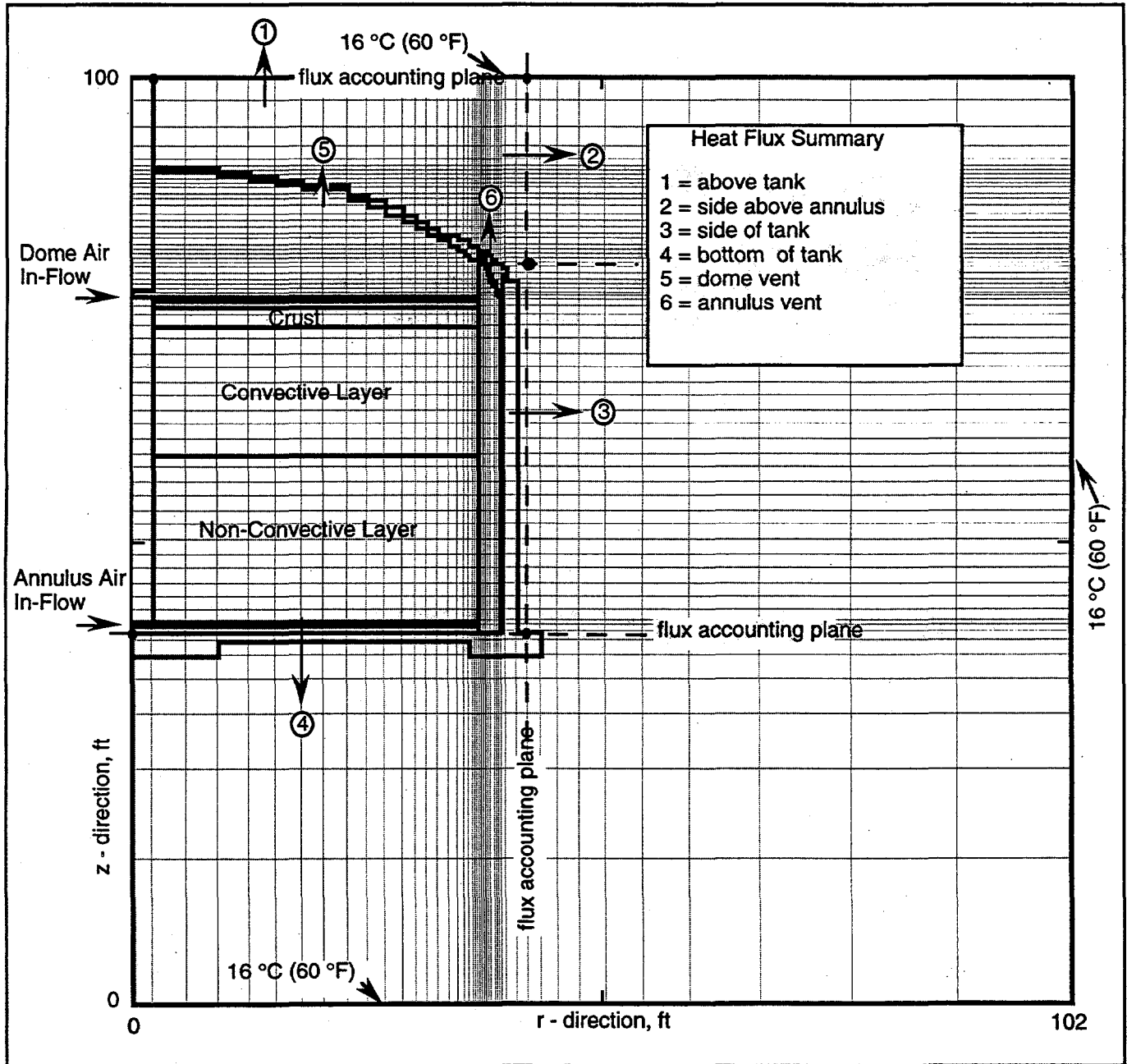


Figure 4.1. Schematic of the Model Domain

Table 4.1. Summary of Conditions and Material Properties for Tank AN-105

	Waste Layer Depth cm (in.)	Density kg/m ³ (lbm/ft ³)	Thermal Conductivity W/m-K (Btu/ft-hr-°F)	Specific Heat kJ/kg-K (Btu/lbm-°F)	Viscosity cP (lbm/ft-s)	Volumetric Heat Generation Rate W/m ³ (Btu/ft ³ -hr)
Crust	8 (3)	1,345 (84) ^(a)	1.4 (0.8)	1.3 (0.3)	solid	1.72 (0.166)
Convective Layer	554 (218)	1,430 (89)	0.61 (0.35)	4.2 (0.99)	36 (0.024)	1.72 (0.166)
Nonconvective Layer	457 (180)	1,590 (99)	1.4 (0.8)	2.4 (0.57)	solid	1.72 (0.166)
Total	980 (386)					
Insulating concrete		2,250 (140)	0.23 (0.13)	2.0 (0.2)		
Steel		7,860 (490)	47 (27)	1.1 (0.11)		
Concrete in Walls		2,250 (140)	0.93 (0.54)	2.0 (0.2)		
Earth		1,600 (100)	0.78 (0.45)	4.5 (0.44)		

(a) Assumed, based on data from similar tanks.

An initial temperature profile based on recent thermocouple readings was assumed, and a constant, uniform heat generation rate was imposed within the waste. It was assumed that this heat generation rate was 7.42 kW (25,000 Btu/hr), an intermediate value that has been reported for AN-105 (Jo 1997).

Heat transfer at the convective/nonconvective and convective/tank shell interfaces is determined by the combination of cell-to-cell conduction with heat/mass transfer associated with fluid motion (Trent and Eyler 1997). Buoyancy-driven flow in the convecting waste carries heat to the waste extremities. Heat is conducted through the crust and nonconvective waste and through the tank walls and concrete, while air flowing over the inner tank shell and crust surface removes heat from the tank via air exhaust vents. Heat radiates from the crust surface to the dome and between the tank shells in the annulus and is conducted through the surrounding earth.

An exact measurement of vent air flow for AN-105 does not exist. Dome inflow was estimated to be 2.8 m³/min (100 cfm)^(a). The annulus flow rate was estimated to be 5.7 m³/min (200 cfm) from exhauster flow measurements, assuming that there is equal flow through the tanks on this exhauster (Tanks AN-104 through AN-107 share a single, common exhauster). Note that the maximum design annulus air flow rate for AN-105 is 22.7 m³/min (800 cfm)^(a). Based on

(a) Nicholson RS (LMHC). December 20, 1997. Personal communication.

modeling SY-101, ^(a) an annual average of 16°C (60°F) was used as the inflow temperature for both the primary tank (dome) and annulus regions. The effect of seasonal variations on waste temperature is quite small, about 1°C (2°F) based on SY-101 temperature history. ^(b)

Convective heat transfer coefficients for the bottom air channels are average values for each of the three lengths of channel extending from the center manifold to the annulus. Coefficients used in the final simulation are listed in Table 4.2.

Table 4.2. Bottom Air Channel Heat Transfer Coefficients

Tank	Annulus Flow Rate, m ³ /min (cfm)	Heat Transfer Coefficient W/m ² -K (Btu/h ft ² °F)		
		Innermost Channel	Mid-Channel	Outermost Channel
AN-105	5.7 (200)	4.7 (0.83)	5.5 (0.96)	6.5 (1.14)

4.2 Parametric Study to Determine Initial Conditions (steady state)

Several simulations of the thermal state of Tank AN-105 were needed to converge on a solution because actual airflow rates in AN-105 are uncertain. In addition, a range of heat loads are reported for AN-105 (Jo 1997). Four "initial condition" cases were run, as summarized in Table 4.3. Cases 1 and 2 were not run to a fully converged solution because intermediate results indicated that the selected annulus air flow rates were much too high, resulting in calculated temperatures that were much lower than measured.

Figure 4.2 shows the results from Case 4 and compares them with actual tank temperatures measured on December 28, 1997 at the MIT in riser 15A. The temperatures measured by an old thermocouple tree in riser 4A parallel the MIT temperatures but are slightly higher. Given the uncertainties in temperature measurements and in waste retrieval scenarios, it was felt that Case 4 adequately represented current tank waste hydrothermal conditions. Note that some of the differences between the measured and the calculated results are because the TEMPEST code uses average annual air temperature as input, indicative of a steady-state condition, while the real data represent winter conditions and it is unlikely that the tank is actually at steady state.

Figure 4.3 displays the Case 4 results in the form of temperature contours, taken in a vertical plane through the tank (because of symmetry, only one-half of the tank is actually shown). Note the cooler regions, both above and below the waste, that are partially determined by the vent air flow rates and temperatures. Also note that the hottest, nonconvective waste temperature forms a torus due to the central inflow of annulus cooling air via channels below the tank bottom.

(a) Antoniak ZI. 1994. *Study of Tank 241-SY-101 Thermal Behavior Using the TEMPEST Code*. PNLMIT:030394, Pacific Northwest National Laboratory, Richland, Washington

(b) Antoniak ZI and KP Recknagle. 1995. *Detailed Studies of Tank 241-SY-101 Thermal Behavior Using the TEMPEST Code*. PNLMIT:072595, Pacific Northwest National Laboratory, Richland, Washington.

Table 4.3. Results of the Annulus Air Flow Sensitivity Analysis

Case	Annulus Flow Rate, m ³ /min. (cfm)	Maximum Temperature, °C (°F)	Convective Waste Temperature, °C (°F)
1	22.7 (800)	n/a (not converged)	n/a (not converged)
2	11.3 (400)	n/a (not converged)	n/a (not converged)
3	8.50 (300)	38.1 (100.6)	32.6 (90.7)
4	5.66 (200)	40.4 (104.7)	34.5 (94.1)

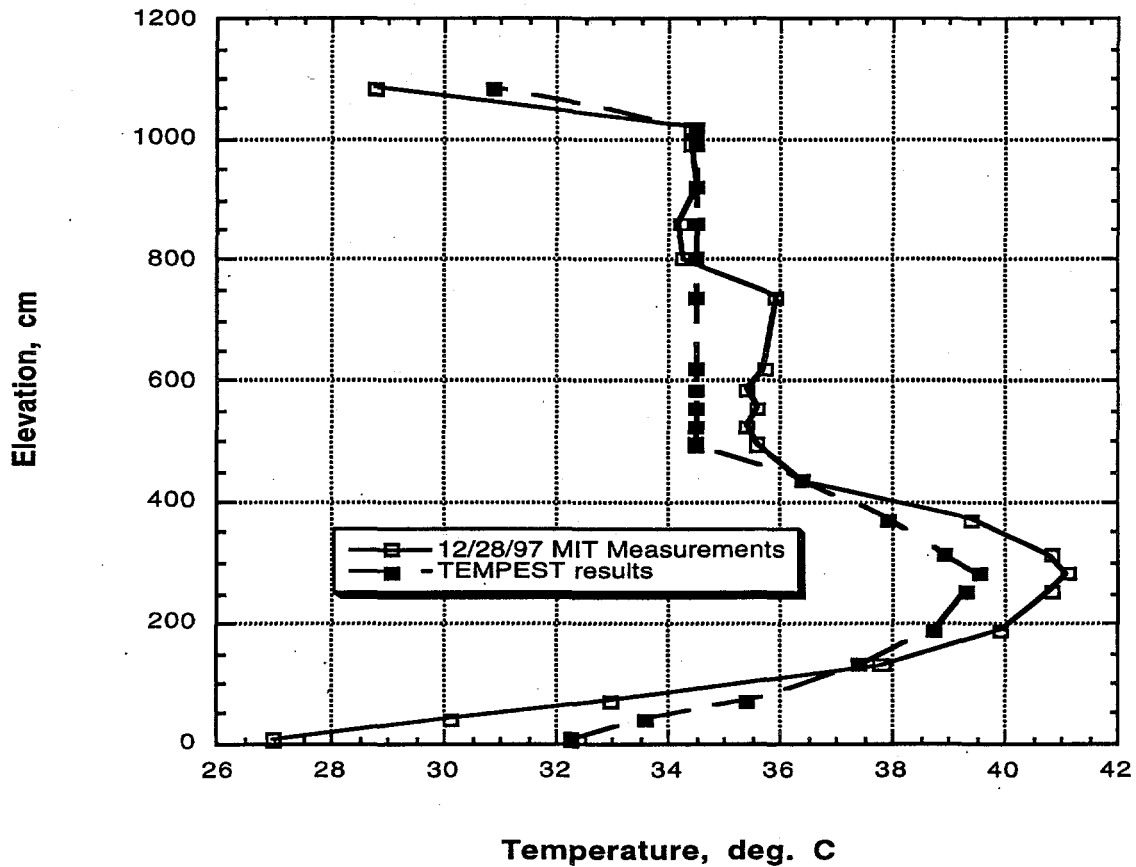


Figure 4.2. Measured and Calculated Temperature Comparison for Tank AN-105

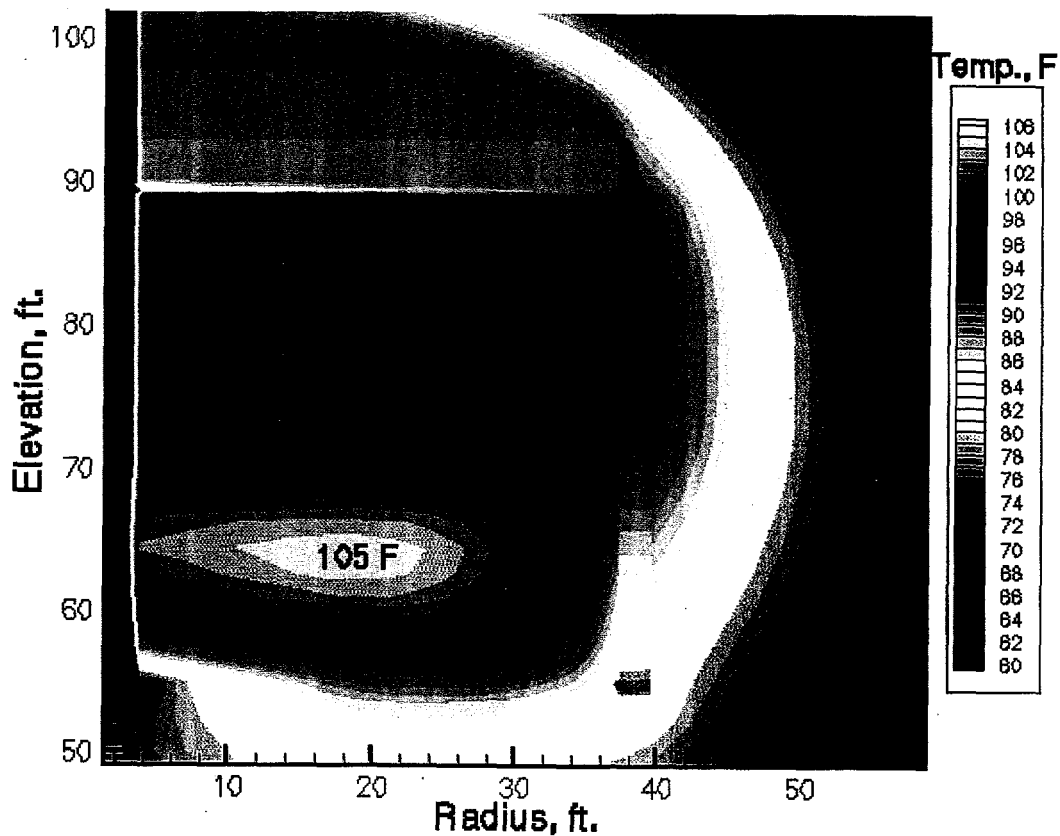


Figure 4.3. Calculated Steady-State Temperature Contours for Tank AN-105

4.3 Simulation of the Cooldown of a Hot, Mixed Tank (transient)

It was assumed that prior to retrieval activities, the tank waste would be fully mixed, both vertically and horizontally, to a uniform consistency and a uniform temperature of 82.2°C (180°F). This scenario was initially suggested as a method for dissolving some of the waste solids by elevating the temperature. The waste temperature would be raised by input energy from the two 300-hp pumps running continuously for several weeks. It was further assumed that the mixing period would be sufficiently brief so that the boundary (earth, tank structure) temperatures would not be affected. The simulation was started with the execution of a short, fully-transient run, with all waste at 82.2°C, with the waste structure as before (this assumes that the settling of the waste solids is rapid with respect to the thermal time constant, especially in rebuilding the nonconvective layer, which is consistent with the waste particle size distribution,^(a) and with all other temperatures started at the values obtained from the final steady-state run (Case 4) as discussed in Section 4.2. Only very small temperature changes occurred during this transient, but velocities (convective

(a) Onishi Y (PNNL). January 14, 1998. Personal communication.

waste, dome, and annulus air) changed significantly from the steady-state run and stabilized. The simulation was continued, but all the velocities were fixed to accelerate the transient heat transfer solution for an (assumed) 180-day cooldown period; even with this simplification, about one day of cpu time was required to model ~ 10 days of "real time."

Figure 4.4 shows the transient temperatures for AN-105 during the 180-day cooldown period. The cooldown of the waste proceeded monotonically, except for a slight heatup of the nonconvective waste to ~83.3°C (~182°F) from the internal heat generated. The temperatures for a cell about 0.3 m (1ft) into the earth, at the same elevation of the nonconvective waste cell shown, is also plotted in Figure 4.4. The earth surrounding the tank warmed appreciably during the first 50 days of the transient and then remained fairly constant. At the end of the 180-day cooldown period, the tank contents remained quite hot, with the nonconvective waste peak temperature at 76°C (169°F), and the convective waste at a near-uniform 62°C (143°F).

A second transient simulation was performed, assuming again that the entire tank contents were at a uniform temperature of 82.2°C (180°F). However, for this case, the thickness of the nonconvective waste layer was assumed to equal the original AN-105 nonconvective layer depth

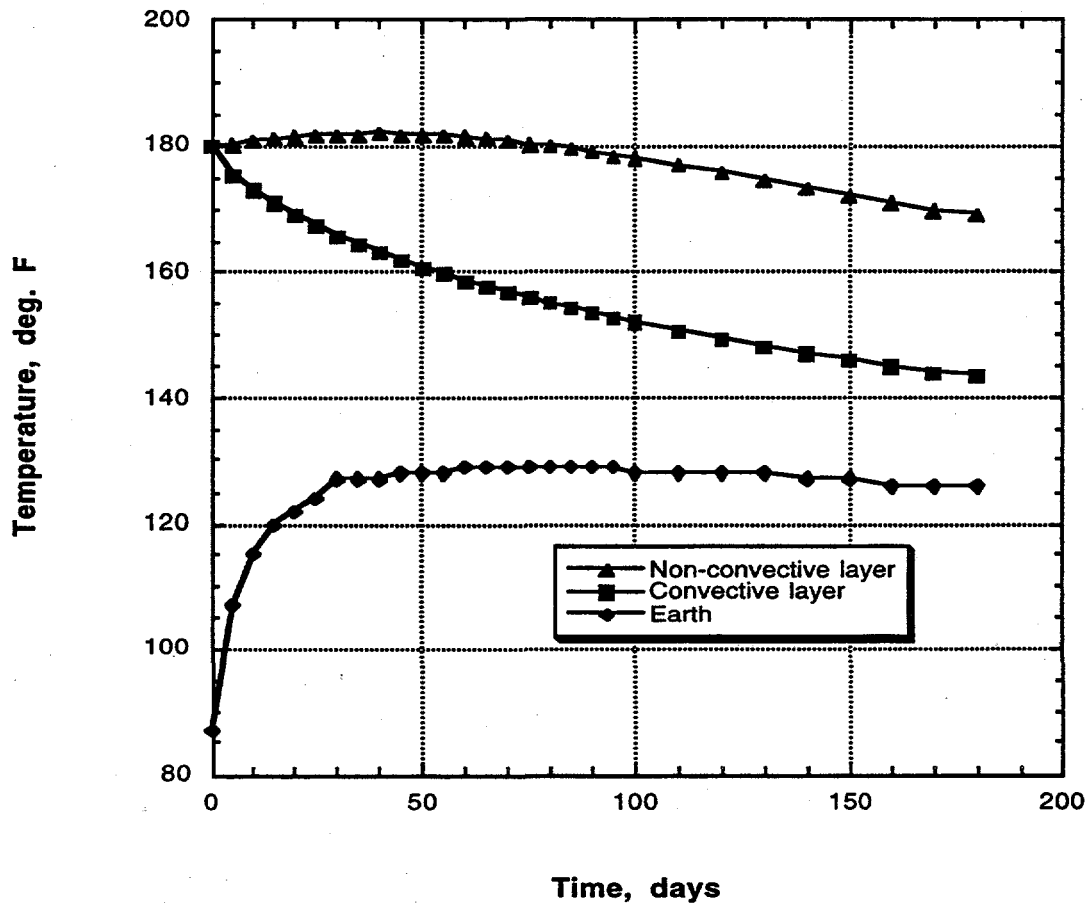


Figure 4.4. Calculated Transient Temperatures for Tank AN-105 Cooldown

multiplied by a "fluff" factor of 1.8. The reason for assuming a fluff factor is that after mixing, tank waste does not settle to the same level it was prior to mixing because of entrained liquid. It can take several months, even up to a year, before the waste level is reduced to its original height. Bench-scale tests and computer simulations of other tanks suggest that the nonconvective volume increase may be in the range of 1.4 to 1.8 times the original volume (Reynolds 1997). This increase in volume increases the thermal conduction path length through the nonconvective waste and therefore has a large impact on calculated temperatures.

The transient temperature profiles for the run with a 1.8 fluff factor parallel those shown in Figure 4.4, except that the nonconvective layer temperature rose to a peak of nearly 86.1°C (186.9°F) after 150 days of cooling. At the end of the 180-day cooldown period, the tank contents remained quite hot, with the nonconvective waste peak temperature at 85.9°C (186.6°F) and the convective waste at a near-uniform 48°C (119°F).

4.4 Simulation of Steady-State after Supernatant Decant

The second retrieval scenario simulated a tank in which the convective/supernatant layer was decanted so the only remaining waste in the tank was the original nonconvective layer. This scenario could occur during an unplanned delay in dilution following supernatant decant. There is some concern that the absence of liquid might produce high temperatures in the waste. The model required some alteration, in the form of cell size changes, to preserve the finer structure required near interfaces to correctly model radiation and convective heat transfer. This simulation was run to a steady state, with all properties and other assumptions the same as in earlier runs (see Sections 4.2 and 4.3). The resulting temperatures are presented in the upper frame of Figure 4.5 in the form of contours in a vertical plane through the waste. The hot torus is still evident but, as expected, the peak temperature has declined some 8°C (14°F) from the full-tank condition (compare with Figure 4.3). Three additional sensitivity runs were also performed; 2 cases of "fluffed" waste after supernatant decant and one case with "fluffed" waste prior to supernatant decant. The results from the simulation of a decanted tank with a "fluff factor" of 1.4 are shown in the lower frame of Figure 4.5. Figure 4.6 compares the results from two simulations with a "fluff factor" of 1.8; the upper frame shows the results of a decanted tank and the lower frame shows the results of a tank prior to supernatant decant.

As indicated above, the upper contour map in Figure 4.5 represents a tank with 457 cm (180 in.) of nonconvective waste (it was assumed that the convective layer had previously been decanted). The peak waste temperature for this simulation was 32.6°C (90.7°F). The lower contour map simulates the same decanted tank condition, except a "fluff factor" of 1.4 was applied to the waste, resulting in a nonconvective waste depth of $457 \times 1.4 = 640$ cm (252 in.) (note that all properties were unaltered except for increased waste volume). This simulation had a peak waste temperature of 42.2°C (108°F).

The upper contour map in Figure 4.6 is similar to those in Figure 4.5, except that in this case a "fluff factor" of 1.8 was used, resulting in a nonconvective waste depth of 822.6 cm (324 in.) and a peak waste temperature of 53.1°C (127.6°F). The lower contour map in Figure 4.6 also has a

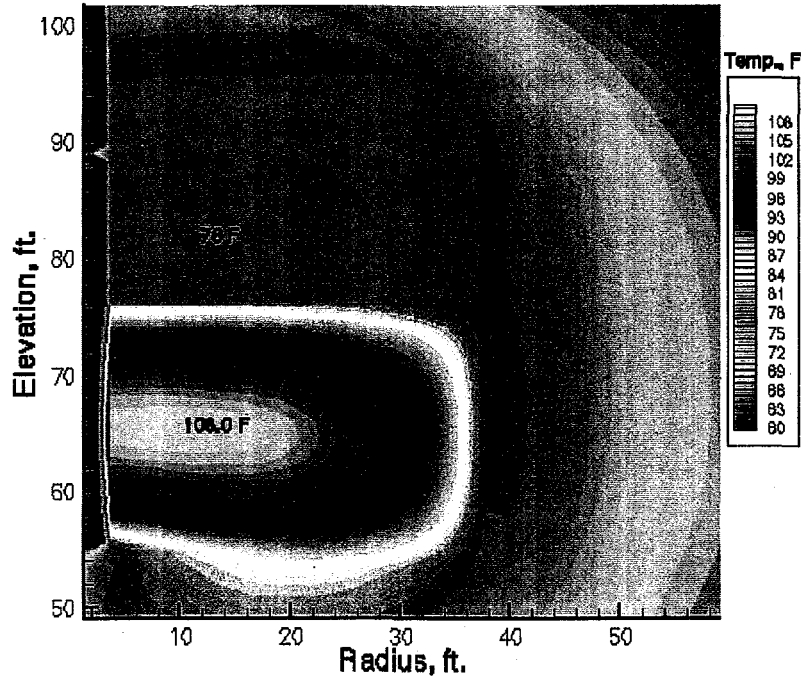
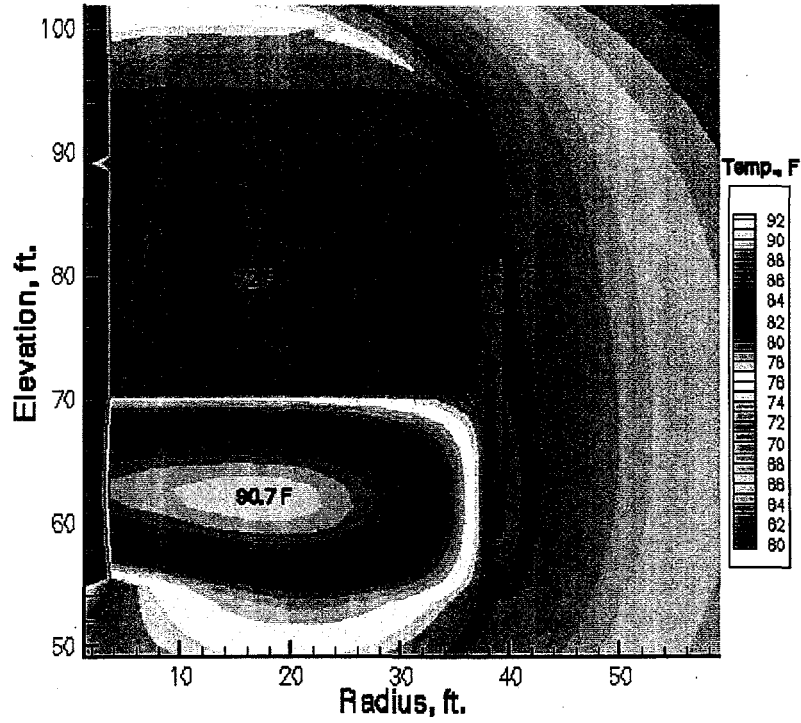


Figure 4.5. Calculated Steady-State Temperature Contours for AN-105 Waste After Supernatant Decant; Upper Frame = "Fluff Factor" of 1, Lower Frame = "Fluff Factor" of 1.4

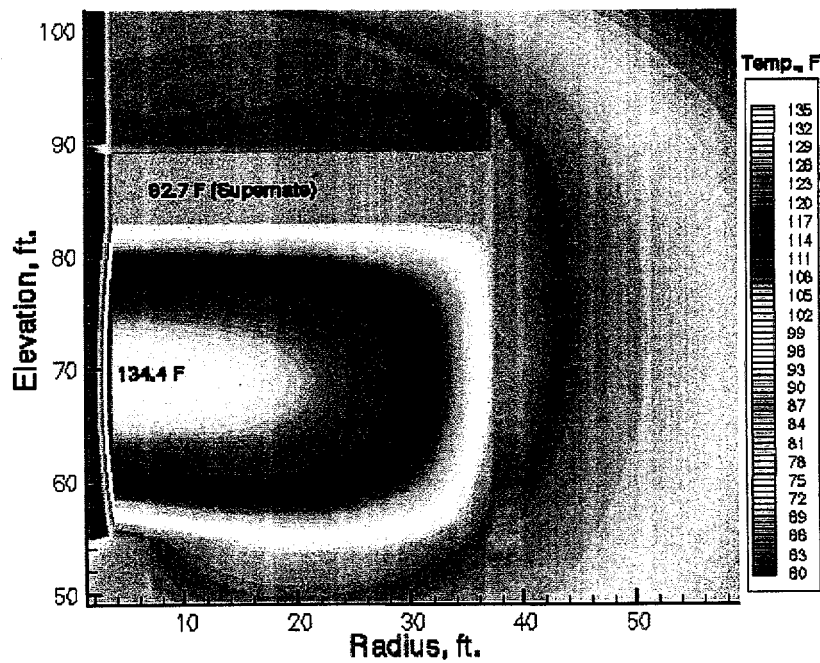
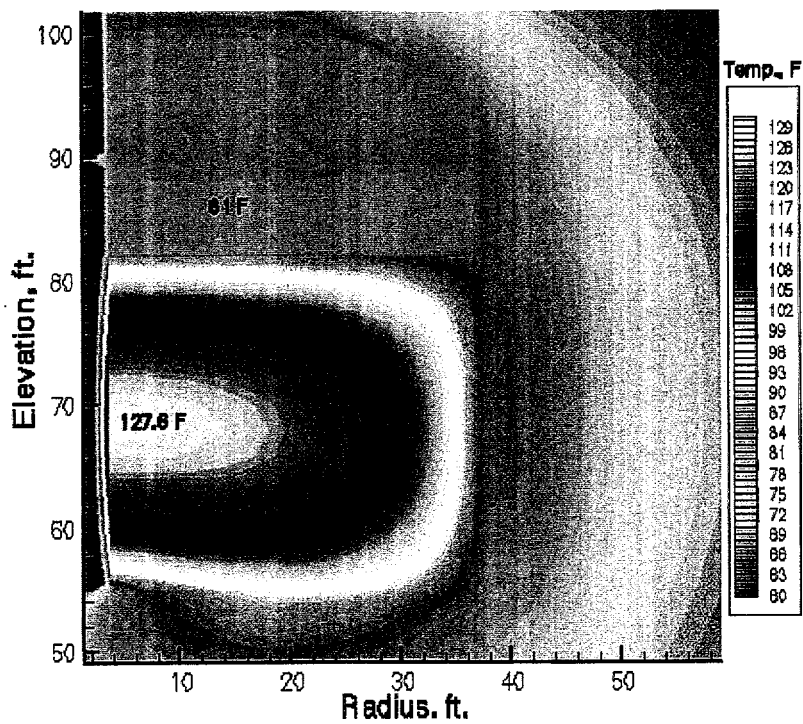


Figure 4.6. Calculated Steady-State Temperature Contours for AN-105 Waste with a “Fluff Factor” of 1.8; Upper Frame = After Supernatant Decant, Lower Frame = Before Supernatant Decant

"fluff" of 1.8 but represents a tank with the supernatant still in place (i.e., it was not previously decanted), so the total waste height is 1,041 cm (410 in.). Peak temperatures for this case were 56.9°C (134.4°F) in the nonconvective waste and 33.7°C (92.7°F) in the convective waste layer. The nonconvective waste was about 4°C (7°F) hotter for this case than for the earlier case (upper frame, Figure 4.6) where the supernatant was decanted. Note also that the peak temperature shifts inward radially (toward the tank center) with increasing "fluff" factor, as the waste is less influenced by the cooling annulus flow. As expected, the highest nonconvective waste temperature occurs for the case with the highest assumed "fluff" of 1.8 and prior to any supernatant decant (lower frame of Figure 4.6).

4.5 Summary and Conclusions

Initial steady-state thermal modeling of AN-105 behavior has resulted in temperatures that closely correspond to measured values. This suggests that the assumptions in this thermal model regarding waste composition, properties, and vent air flows are valid and that the knowledge of this tank is sufficient for the purpose of these analyses. The two analyses that were performed showed that:

1. The transient cooling of the waste, from a uniform 82.2°C (180°F), over a 180-day period is initially rapid as the waste heats up the surrounding earth, but slows thereafter. The tank remains quite hot, even after a six-month period. Cooling is slower, and the peak nonconvective waste temperature is slightly higher for a "fluffed" waste.
2. The steady-state temperatures of the waste remaining after supernatant decant are low, with peak waste temperatures between ~33 and 53°C (91 and 128°F), depending on the amount of "fluff." If decant does not take place after mixing, the peak waste temperature for a 1.8 "fluff" case is calculated to be approximately 57°C (134°F).

5.0 References

Allemann RT, TM Burke, DA Reynolds, and DE Simpson. 1993. *Assessment of Gas Accumulation and Retention - Tank 241-SY-101*. WHC-EP-0576 Rev. 0, Westinghouse Hanford Company, Richland, Washington.

Allemann RT, ZI Antoniak, WD Chvala, LE Efferding, JG Fadeff, JR Friley, WB Gregory, JD Hudson, JJ Irwin, NW Kirch, TE Michener, FE Panisko, CW Stewart, and BM Wise. 1994. *Mitigation of Tank 241-SY-101 by Pump Mixing: Results of Testing Phases A and B*. PNL-9423, Pacific Northwest National Laboratory, Richland, Washington.

Antoniak ZI. 1993. *Historical Trends in Tank 241-SY-101 Waste Temperatures and Levels*. PNL-8880, Pacific Northwest National Laboratory, Richland, Washington.

Babad H, GD Johnson, and DA Reynolds. 1992. *Understanding the Cyclic Venting Phenomena in Hanford Site High-Level Waste Tanks: The Evaluation of Tank 241-SY-101*. WHC-SA-1364-FP, Westinghouse Hanford Company, Richland, Washington.

Brewster, ME, NB Gallagher, JD Hudson, and CW Stewart. 1995. *The Behavior, Quantity, and Location of Undissolved Gas in Tank 241-SY-101*. PNL-10681, Pacific Northwest Laboratory, Richland, Washington.

Cashdollar KL, M Hertzberg, IA Zlochower, CE Lucci, GM Green, and RA Thomas. 1992. *Laboratory Flammability Studies of Mixtures of Hydrogen, Nitrous Oxide, and Air*. WHC-SD-WM-ES-219, Westinghouse Hanford Company, Richland, Washington.

Chhabra RP and PHT Uhlherr. 1986. "Static Equilibrium and Motion of Spheres in Viscoplastic Liquids." *Encyclopedia of Fluid Mechanics*, Vol. 21, NP Cheremisinoff (ed.), pp. 611-633.

Hanlon BM. 1995. *Waste Tank Summary Report for Month Ending August 31, 1995*. WHC-EP-0182-89, Westinghouse Hanford Company, Richland, Washington.

Hanlon BM. 1998. *Waste Tank Summary Report for Month Ending January 31, 1998*. HNF-EP-0182-118, Lockheed Martin Services Inc., Richland, Washington.

Herting DL, TL Welsh, RW Lambie, and TT Tran. 1995. *Tank Characterization Report for Double Shell Tank 241-SY-101*. WHC-SD-WM-ER-409 Rev. 0, Westinghouse Hanford Company, Richland, Washington.

Herting DL. 1997. *Results of Dilution Studies with Waste from Tank 241-AN-105*. HNF-SD-WM-DTR-046 Rev. 0, Numatec Hanford Corp., Richland, Washington.

Hu, TA. 1997. *Calculations of Hydrogen Release Rate at Steady State for Double-Shell Tanks*. HNF-SD-WM-CN-117 Rev. 0, Lockheed Martin Hanford Corp., Richland, Washington.

Jo J. 1997. *Tank Characterization Report for Double Shell Tank 241-AN-105*. WHC-SD-WM-ER-678 Rev. 0A, Westinghouse Hanford Company, Richland, Washington.

King CM, LR Pederson, and SA Bryan. 1997. *Thermal and Radiolytic Gas Generation from Tank 241-S-102 Waste*. PNNL-11600, Pacific Northwest National Laboratory, Richland, Washington.

Kubic, WL Jr., G. Pillay. 1997. *Data Reconciliation Study of Tank AN-105 at the Hanford Site*. LA-UR-97-3916, Los Alamos National Laboratory, Los Alamos, New Mexico.

Mahoney LA, ZI Antoniak, and JM Bates. 1997. *Composition and Quantities of Retained Gas Measured in Hanford Waste Tanks 241-U-103, S-106, BY-101, and BY-109*. PNNL-11777, Pacific Northwest National Laboratory, Richland, Washington.

Meyer PA, ME Brewster, SA Bryan, C Chen, LR Pederson, CW Stewart, and G Terrones. 1997. *Gas Retention and Release Behavior in Hanford Double-Shell Waste Tanks*. PNNL-11536 Rev. 1, Pacific Northwest National Laboratory, Richland, Washington.

Norton, JD, LR Pederson. 1995. *Solubilities of Gases in Simulated Tank 241-SY-101 Wastes*. PNL-10785, Pacific Northwest Laboratory, Richland, Washington.

Peurrung, LM, LA Mahoney, CW Stewart, PA Gauglitz, LR Pederson, SA Bryan, and CL Shepard. 1998. *Flammable Gas Issues in Double-Contained Receiver Tanks*. PNNL-11836 Rev. 2, Pacific Northwest National Laboratory, Richland, Washington.

Reynolds, DA. 1994. *Evaluation of 241 AN Tank Farm Flammable Gas Behavior*. WHC-EP-0717, Westinghouse Hanford Company, Richland, Washington.

Reynolds, DA. 1997. *Chemical and Chemically Related Considerations Associated with Sluicing Tank C-106 Waste to Tank AY-102*. HNF-SD-WM-TI-756 Rev. 1, Lockheed Martin Hanford Corp., Richland, Washington.

Shekarriz A, DR Rector, LA Mahoney, MA Chieda, HM Bates, RE Bauer, NS Cannon, BE Hey, CG Linschooten, FJ Reitz, and ER Siciliano. 1997. *Composition and Quantities of Retained Gas Measured in Hanford Waste Tanks 241-AW-101, A-101, AN-105, AN-104, and AN-103*. PNNL-11450 Rev. 1, Pacific Northwest National Laboratory, Richland, Washington.

Stewart CW, JD Hudson, JR Friley, FE Panisko, ZI Antoniak, JJ Irwin, JG Fadeff, LF Efferding, TE Michener, NW Kirch, and DA Reynolds. 1994. *Mitigation of Tank 241-SY-101 by Pump Mixing: Results of Full-Scale Testing*. PNL-9959, Pacific Northwest National Laboratory, Richland, Washington.

Stewart, CW, JM Alzheimer, ME Brewster, G Chen, RE Mendoza, HC Reid, CL Shepard, and G Terrones. 1996. *In Situ Rheology and Gas Volume in Hanford Double-Shell Waste Tanks* PNNL-11296, Pacific Northwest National Laboratory, Richland, Washington.

Sullivan HL. 1995. *A Safety Assessment for Proposed Pump Mixing Operations to Mitigate Episodic Gas Releases in Tank 241-SY-101: Hanford Site, Richland, Washington*. HNF-SD-WM-SAD-033 Rev. 3, U.S. Department of Energy, Richland, Washington.

Trent DS and LL Eyler. 1997. *TEMPEST - A Computer Program for Three-Dimensional Time-Dependent Computational Fluid Dynamics and Hydrothermal Analysis*. PNNL-4348 Vol. 1, Rev. 4, Pacific Northwest National Laboratory, Richland, Washington.

Wilkins NE, RE Bauer, and DM Ogden. 1997. *Results of Vapor Space Monitoring of Flammable Gas Watch List Tanks*. HNF-SD-WM-TI-797 Rev. 2, Lockheed Martin Hanford Company, Richland, Washington.

Distribution

<u>No. of Copies</u>		<u>No. of Copies</u>	
2	<u>Office of Scientific and Technical Information</u>	21	<u>Pacific Northwest National Laboratory</u>
1	<u>DOE Richland Operations Office</u>		Z. I. Antoniak K7-15
	J. L. Davis L7-12		S.Q. Bennett K7-90
			S. M. Caley K6-28
			J. M. Cuta K7-15
			J. A. Fort K7-15
10	<u>PHMC Team</u>		P. A. Gauglitz K6-28
	J. E. Van Beek (4) S2-48		W. L. Kuhn K8-93
	P. J. Certa R3-73		L. A. Mahoney K7-15
	A. F. Choho H6-35		P. A. Meyer K7-15
	E. W. Leschber B1-42		Y. Onishi K9-33
	R. P. Marshall R3-74		F. E. Panisko K8-34
	C. A. Rieck S2-48		C. W. Stewart (5) K7-15
	W. T. Thompson R3-73		Information Release (5) K6-06